CosmoInformatics

Sparsity, wavelets, compressive sensing and all that. . .

Jason McEwen
www.jasonmcewen.org
@jasonmcewen

Mullard Space Science Laboratory (MSSL)
University College London (UCL)

MSSL Astro Seminar, Mar 2014

What is sparsity?

— representation of data in such a way that many data points are zero

What is sparsity?

What is sparsity?

Sparsifying transform

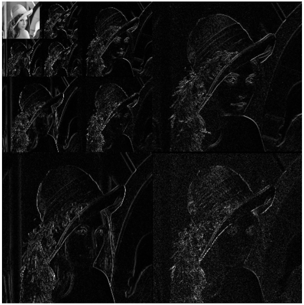

Why is sparsity useful?

— efficient characterisation of structure

Why is sparsity useful?

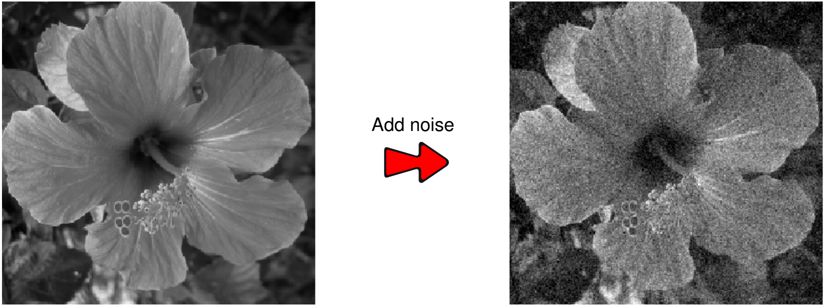

Why is sparsity useful?

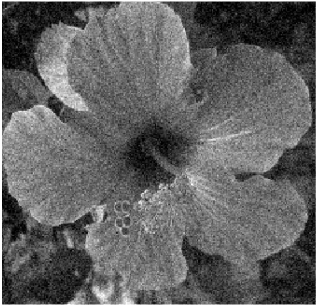

Sparsifying transform

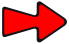

Why is sparsity useful?

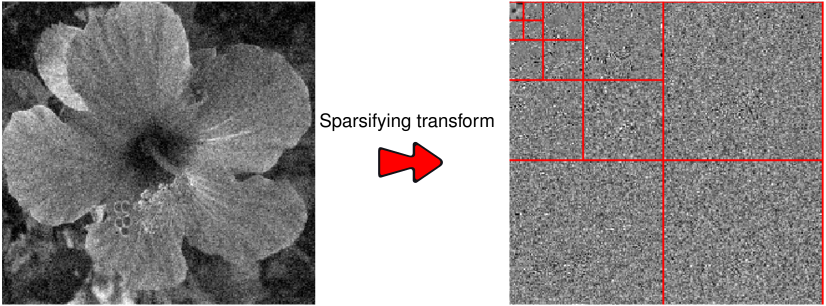

Why is sparsity useful?

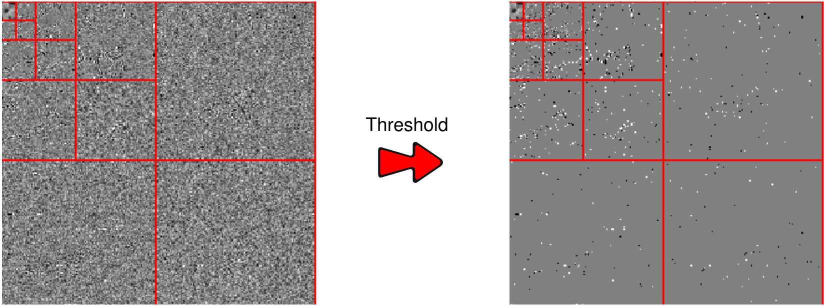

Why is sparsity useful?

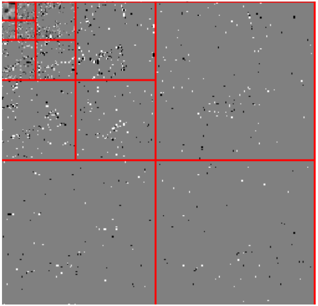

Why is sparsity useful?

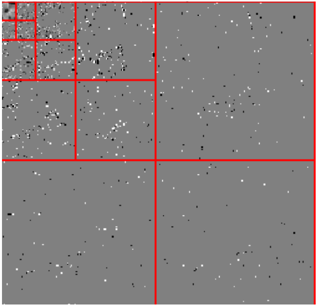

Inverse transform

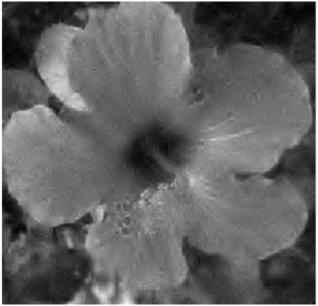

Why is sparsity useful?

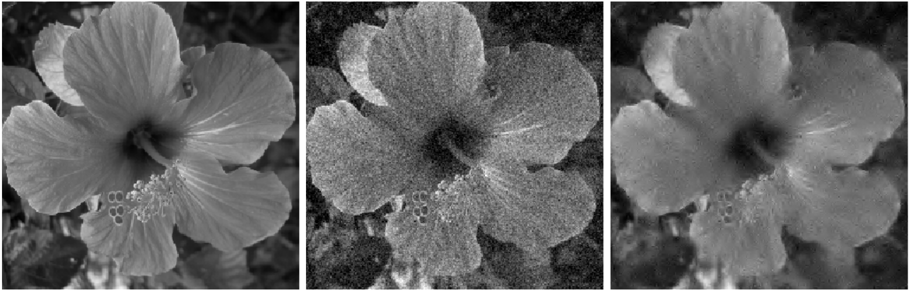

(a) Original (b) Noisy (c) Denoised

[Credit: http://www.ceremade.dauphine.fr/~peyre/numerical-tour/tours/denoisingwav_2_wavelet_2d/]

How can we construct sparsifying transforms?

— many signals in nature have spatially localised, scale-dependent features

How can we construct sparsifying transforms?

Fourier (1807)

Haar (1909)

Morlet and Grossman (1981)

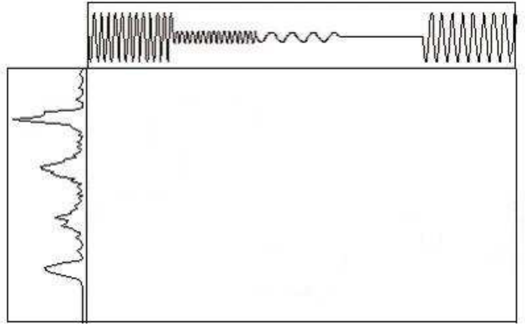

Figure: Fourier vs wavelet transform [Credit: `http://www.wavelet.org/tutorial/`]

How can we construct sparsifying transforms?

Fourier (1807)

Haar (1909)

Morlet and Grossman (1981)

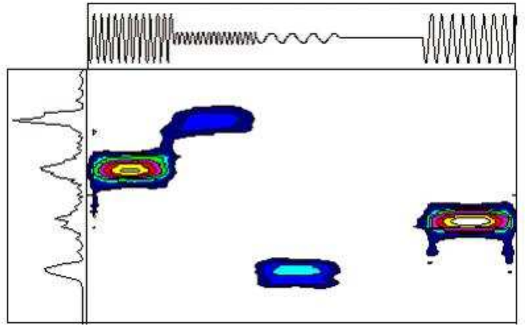

Figure: Fourier vs wavelet transform [Credit: http://www.wavelet.org/tutorial/]

How can we construct sparsifying transforms?

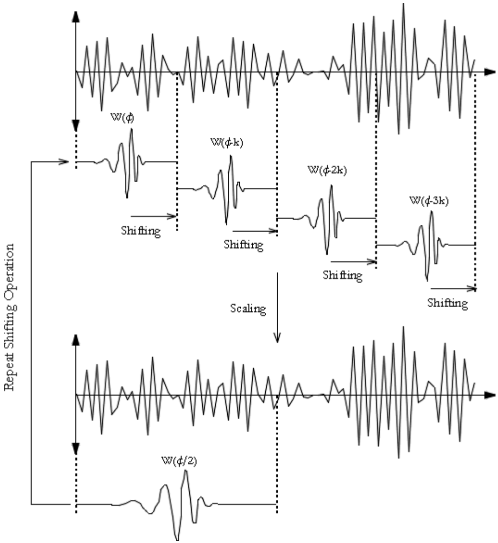

Figure: Wavelet scaling and shifting [Credit: `http://www.wavelet.org/tutorial/`]

Observations on the celestial sphere in cosmology

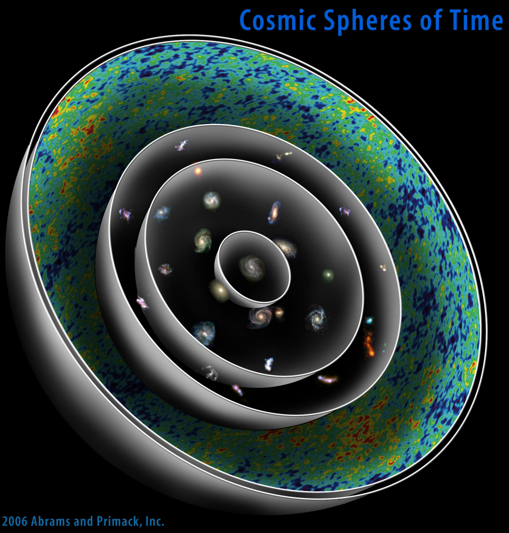

Outline

Dark energy

- Universe consists of ordinary baryonic matter, cold dark matter and dark energy.
- Dark energy represents energy density of empty space, which acts as a repulsive force.
- Strong evidence for dark energy exists but we know very little about its nature and origin.
- A consistent model in the framework of particle physics lacking.

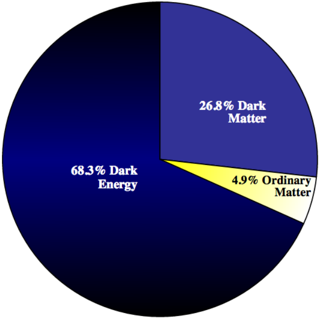

Figure: Content of the Universe [Credit: Planck]

Dark energy

- Universe consists of ordinary baryonic matter, cold dark matter and dark energy.
- Dark energy represents energy density of empty space, which acts as a repulsive force.
- Strong evidence for dark energy exists but we know very little about its nature and origin.
- A consistent model in the framework of particle physics lacking.

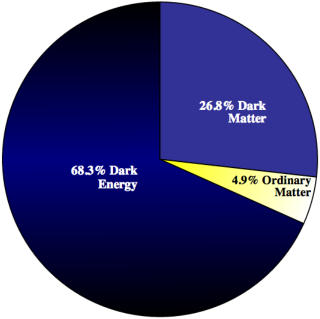

Figure: Content of the Universe [Credit: Planck]

Integrated Sachs Wolfe Effect

Analogy

(no dark energy)

(with dark energy)

(a) No dark energy

(b) With dark energy

Figure: Analogy of ISW effect

Integrated Sachs Wolfe Effect

Correlation between CMB and LSS

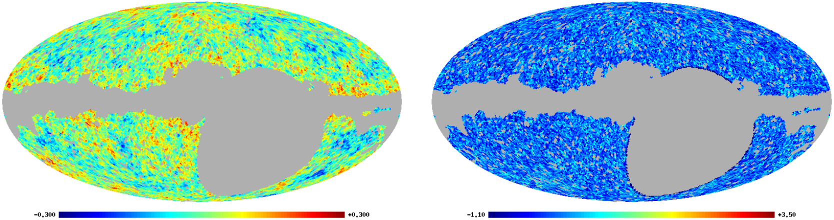

(a) CMB (b) LSS

Figure: Constraining dark energy through any correlation between the CMB and LSS.

Recall wavelet transform in Euclidean space

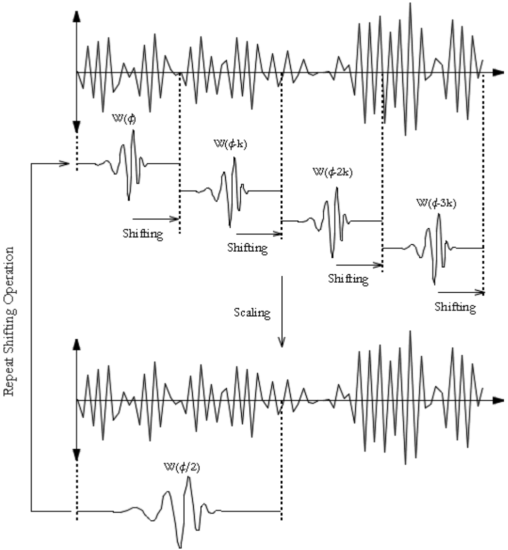

Figure: Wavelet scaling and shifting [Credit: http://www.wavelet.org/tutorial/]

Continuous wavelets on the sphere

- One of the first natural wavelet construction on the sphere was derived in the seminal work of Antoine and Vandergheynst (1998) (reintroduced by Wiaux 2005).
- Construct wavelet atoms from affine transformations (dilation, translation) on the sphere of a mother wavelet.
- The natural extension of translations to the sphere are rotations. Rotation of a function f on the sphere is defined by

$$\underbrace{[\mathcal{R}(\rho)f](\omega) = f(\rho^{-1}\cdot\omega), \quad \omega = (\theta,\varphi) \in \mathbb{S}^2, \quad \rho = (\alpha,\beta,\gamma) \in \mathrm{SO}(3)\,.}_{\text{translation}}$$

- How define dilation on the sphere?
- The spherical dilation operator is defined through the conjugation of the Euclidean dilation and stereographic projection Π:

$$\underbrace{\mathcal{D}(a) \equiv \Pi^{-1}\, d(a)\, \Pi\,.}_{\text{dilation}}$$

Continuous wavelets on the sphere

- One of the first natural wavelet construction on the sphere was derived in the seminal work of Antoine and Vandergheynst (1998) (reintroduced by Wiaux 2005).
- Construct wavelet atoms from affine transformations (dilation, translation) on the sphere of a mother wavelet.
- The natural extension of translations to the sphere are rotations. Rotation of a function f on the sphere is defined by

$$\boxed{[\mathcal{R}(\rho)f](\omega) = f(\rho^{-1} \cdot \omega), \quad \omega = (\theta, \varphi) \in \mathbb{S}^2, \quad \rho = (\alpha, \beta, \gamma) \in \mathrm{SO}(3) \; .}$$

translation

- How define dilation on the sphere?
- The spherical dilation operator is defined through the conjugation of the Euclidean dilation and stereographic projection Π:

$$\boxed{\mathcal{D}(a) \equiv \Pi^{-1} \, d(a) \, \Pi \; .}$$

dilation

Continuous wavelets on the sphere

- One of the first natural wavelet construction on the sphere was derived in the seminal work of Antoine and Vandergheynst (1998) (reintroduced by Wiaux 2005).
- Construct wavelet atoms from affine transformations (dilation, translation) on the sphere of a mother wavelet.
- The natural extension of translations to the sphere are rotations. Rotation of a function f on the sphere is defined by

$$\boxed{[\mathcal{R}(\rho)f](\omega) = f(\rho^{-1} \cdot \omega), \quad \omega = (\theta, \varphi) \in \mathbb{S}^2, \quad \rho = (\alpha, \beta, \gamma) \in \mathrm{SO}(3) \ .}$$

translation

- How define dilation on the sphere?
- The spherical dilation operator is defined through the conjugation of the Euclidean dilation and stereographic projection Π:

$$\boxed{\mathcal{D}(a) \equiv \Pi^{-1}\, d(a)\, \Pi \ .}$$

dilation

Continuous wavelets on the sphere

- One of the first natural wavelet construction on the sphere was derived in the seminal work of Antoine and Vandergheynst (1998) (reintroduced by Wiaux 2005).
- Construct wavelet atoms from affine transformations (dilation, translation) on the sphere of a mother wavelet.
- The natural extension of translations to the sphere are rotations. Rotation of a function f on the sphere is defined by

$$\boxed{[\mathcal{R}(\rho)f](\omega) = f(\rho^{-1}\cdot\omega), \quad \omega = (\theta,\varphi) \in \mathbb{S}^2, \quad \rho = (\alpha,\beta,\gamma) \in \mathrm{SO}(3)\,.}$$

translation

- How define dilation on the sphere?
- The spherical dilation operator is defined through the conjugation of the Euclidean dilation and stereographic projection Π:

$$\boxed{\mathcal{D}(a) \equiv \Pi^{-1}\, d(a)\, \Pi\,.}$$

dilation

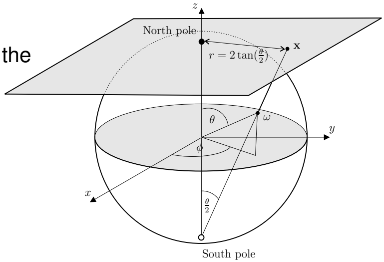

Continuous wavelets on the sphere

Forward transform (*i.e.* analysis)

- Wavelet family on the sphere constructed from rotations and dilations of a mother wavelet Ψ:

$$\boxed{\{\Psi_{a,\rho} \equiv \mathcal{R}(\rho)\mathcal{D}(a)\Psi : \rho \in \mathrm{SO}(3),\, a \in \mathbb{R}_*^+\}\,.}$$

dictionary

- The forward wavelet transform is given by

$$\underbrace{\boxed{W_\Psi^f(a,\rho) = \langle f, \Psi_{a,\rho}\rangle}}_{\text{projection}} = \int_{\mathbb{S}^2} \mathrm{d}\Omega(\omega)\, f(\omega)\, \Psi_{a,\rho}^*(\omega)\,,$$

where $\mathrm{d}\Omega(\omega) = \sin\theta\,\mathrm{d}\theta\,\mathrm{d}\varphi$ is the usual invariant measure on the sphere.

- Wavelet coefficients live in $\mathrm{SO}(3) \times \mathbb{R}_*^+$; thus, directional structure is naturally incorporated.

Continuous wavelets on the sphere

Forward transform (*i.e.* analysis)

- Wavelet family on the sphere constructed from rotations and dilations of a mother wavelet Ψ:

$$\boxed{\{\Psi_{a,\rho} \equiv \mathcal{R}(\rho)\mathcal{D}(a)\Psi : \rho \in \mathrm{SO}(3),\ a \in \mathbb{R}_*^+\}\ .}$$

dictionary

- The forward wavelet transform is given by

$$\boxed{W_\Psi^f(a,\rho) = \langle f, \Psi_{a,\rho}\rangle} \equiv \int_{\mathbb{S}^2} \mathrm{d}\Omega(\omega)\, f(\omega)\, \Psi_{a,\rho}^*(\omega)\ ,$$

projection

where $\mathrm{d}\Omega(\omega) = \sin\theta\, \mathrm{d}\theta\, \mathrm{d}\varphi$ is the usual invariant measure on the sphere.

- Wavelet coefficients live in $\mathrm{SO}(3) \times \mathbb{R}_*^+$; thus, directional structure is naturally incorporated.

Continuous wavelets on the sphere

Forward transform (*i.e.* analysis)

- Wavelet family on the sphere constructed from rotations and dilations of a mother wavelet Ψ:

$$\boxed{\{\Psi_{a,\rho} \equiv \mathcal{R}(\rho)\mathcal{D}(a)\Psi : \rho \in \mathrm{SO}(3),\, a \in \mathbb{R}_*^+\}\,.}$$

dictionary

- The forward wavelet transform is given by

$$\boxed{W_\Psi^f(a,\rho) = \langle f, \Psi_{a,\rho}\rangle} \equiv \int_{\mathbb{S}^2} \mathrm{d}\Omega(\omega)\, f(\omega)\, \Psi_{a,\rho}^*(\omega)\,,$$

projection

where $\mathrm{d}\Omega(\omega) = \sin\theta\,\mathrm{d}\theta\,\mathrm{d}\varphi$ is the usual invariant measure on the sphere.

- Wavelet coefficients live in $\mathrm{SO}(3) \times \mathbb{R}_*^+$; thus, directional structure is naturally incorporated.

Continuous wavelets on the sphere

Fast algorithms

- Fast algorithms essential (for a review see Wiaux, McEwen & Vielva 2007)
  - Factoring of rotations: McEwen *et al.* (2007), Wandelt & Gorski (2001), Risbo (1996)
  - Separation of variables: Wiaux *et al.* (2005)

FastCSWT code `http://www.fastcswt.org`

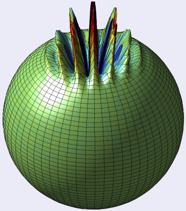

Fast directional continuous spherical wavelet transform algorithms
McEwen *et al.* (2007)

- Fortran
- Supports directional and steerable wavelets

Continuous wavelets on the sphere

Mother wavelets

- Correspondence principle between spherical and Euclidean wavelets (Wiaux *et al.* 2005).
- Mother wavelets on sphere constructed from the projection of mother Euclidean wavelets defined on the plane:

$$\underbrace{\boxed{\Psi = \Pi^{-1}\Psi_{\mathbb{R}^2}}}_{\text{construction}},$$

where $\Psi_{\mathbb{R}^2} \in \mathrm{L}^2(\mathbb{R}^2, \mathrm{d}^2\boldsymbol{x})$ is an admissible wavelet on the plane.

Continuous wavelets on the sphere
Mother wavelets

- Correspondence principle between spherical and Euclidean wavelets (Wiaux *et al.* 2005).
- Mother wavelets on sphere constructed from the projection of mother Euclidean wavelets defined on the plane:

$$\underbrace{\boxed{\Psi = \Pi^{-1}\Psi_{\mathbb{R}^2}}}_{\text{construction}},$$

where $\Psi_{\mathbb{R}^2} \in \mathrm{L}^2(\mathbb{R}^2, \mathrm{d}^2\boldsymbol{x})$ is an admissible wavelet on the plane.

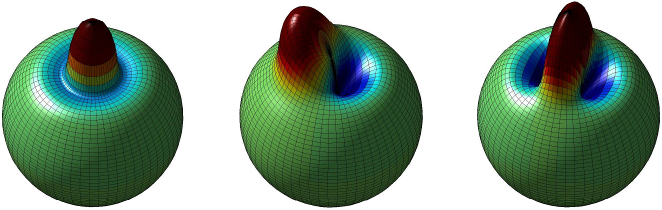

(a) SMHW (b) SBW (c) S2GDW

Figure: Spherical wavelets at scale $a, b = 0.2$.

Continuous wavelets on the sphere

Inverse transform (*i.e.* synthesis)

- The inverse wavelet transform given by

$$f(\omega) = \underbrace{\boxed{\int_0^\infty \frac{\mathrm{d}a}{a^3} \int_{\mathrm{SO}(3)} \mathrm{d}\varrho(\rho)}}_{\text{`sum' contributions}} \underbrace{\boxed{W_\Psi^f(a,\rho)\,[\mathcal{R}(\rho)\widehat{L}_\Psi \Psi_a](\omega)}}_{\text{weighted basis functions}} ,$$

  where $\mathrm{d}\varrho(\rho) = \sin\beta\,\mathrm{d}\alpha\,\mathrm{d}\beta\,\mathrm{d}\gamma$ is the invariant measure on the rotation group $\mathrm{SO}(3)$.

- Perfect reconstruction iff wavelets satisfy admissibility property:

$$0 < \widehat{C}_\Psi^\ell \equiv \frac{8\pi^2}{2\ell+1} \sum_{m=-\ell}^{\ell} \int_0^\infty \frac{\mathrm{d}a}{a^3} \mid (\Psi_a)_{\ell m} \mid^2 < \infty, \quad \forall \ell \in \mathbb{N}$$

  where $(\Psi_a)_{\ell m}$ are the spherical harmonic coefficients of $\Psi_a(\omega)$.

- BUT... exact reconstruction not feasible in practice!

Continuous wavelets on the sphere

Inverse transform (*i.e.* synthesis)

- The inverse wavelet transform given by

$$f(\omega) = \underbrace{\boxed{\int_0^\infty \frac{\mathrm{d}a}{a^3} \int_{\mathrm{SO}(3)} \mathrm{d}\varrho(\rho)}}_{\text{'sum' contributions}} \underbrace{\boxed{W_\Psi^f(a,\rho)\,[\mathcal{R}(\rho)\widehat{L}_\Psi \Psi_a](\omega)}}_{\text{weighted basis functions}} ,$$

where $\mathrm{d}\varrho(\rho) = \sin\beta\,\mathrm{d}\alpha\,\mathrm{d}\beta\,\mathrm{d}\gamma$ is the invariant measure on the rotation group $\mathrm{SO}(3)$.

- Perfect reconstruction iff wavelets satisfy admissibility property:

$$0 < \widehat{C}_\Psi^\ell \equiv \frac{8\pi^2}{2\ell+1} \sum_{m=-\ell}^{\ell} \int_0^\infty \frac{\mathrm{d}a}{a^3} \mid (\Psi_a)_{\ell m} \mid^2 < \infty, \quad \forall \ell \in \mathbb{N}$$

where $(\Psi_a)_{\ell m}$ are the spherical harmonic coefficients of $\Psi_a(\omega)$.

- BUT... exact reconstruction not feasible in practice!

Continuous wavelets on the sphere

Inverse transform (*i.e.* synthesis)

- The inverse wavelet transform given by

$$f(\omega) = \underbrace{\boxed{\int_0^\infty \frac{\mathrm{d}a}{a^3} \int_{\mathrm{SO}(3)} \mathrm{d}\varrho(\rho)}}_{\text{'sum' contributions}} \underbrace{\boxed{W_\Psi^f(a,\rho)\,[\mathcal{R}(\rho)\widehat{L}_\Psi \Psi_a](\omega)}}_{\text{weighted basis functions}} ,$$

  where $\mathrm{d}\varrho(\rho) = \sin\beta\,\mathrm{d}\alpha\,\mathrm{d}\beta\,\mathrm{d}\gamma$ is the invariant measure on the rotation group $\mathrm{SO}(3)$.

- Perfect reconstruction iff wavelets satisfy admissibility property:

$$0 < \widehat{C}_\Psi^\ell \equiv \frac{8\pi^2}{2\ell+1} \sum_{m=-\ell}^{\ell} \int_0^\infty \frac{\mathrm{d}a}{a^3} \mid (\Psi_a)_{\ell m} \mid^2 < \infty, \quad \forall \ell \in \mathbb{N}$$

  where $(\Psi_a)_{\ell m}$ are the spherical harmonic coefficients of $\Psi_a(\omega)$.

- BUT... exact reconstruction not feasible in practice!

Detecting dark energy

Wavelet coefficient correlation

- Compute wavelet correlation of CMB and LSS data
(McEwen *et al.* 2007, McEwen *et al.* 2008).
- Compare to 1000 Monte Carlo simulations.
- Correlation detected at 99.9% significance.

$\Rightarrow$ Independent evidence for the existence of dark energy!

Detecting dark energy

Wavelet coefficient correlation

- Compute wavelet correlation of CMB and LSS data (McEwen *et al.* 2007, McEwen *et al.* 2008).
- Compare to 1000 Monte Carlo simulations.
- Correlation detected at 99.9% significance.

$\Rightarrow$ Independent evidence for the existence of dark energy!

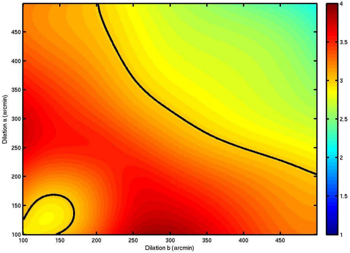

Figure: Wavelet correlation N_σ surface. Contours are shown at 3σ.

Detecting dark energy

Constraining cosmological models

- Use positive detection of the ISW effect to constrain parameters of cosmological models:
  - Energy density Ω_Λ.
  - Equation of state parameter w relating pressure and density of cosmological fluid modelling dark energy, *i.e.* $p = w\rho$.
- Parameter estimates of $\boxed{\Omega_\Lambda = 0.63^{+0.18}_{-0.17}}$ and $\boxed{w = -0.77^{+0.35}_{-0.36}}$ obtained.

Detecting dark energy

Constraining cosmological models

- Use positive detection of the ISW effect to constrain parameters of cosmological models:
    - Energy density Ω_Λ.
    - Equation of state parameter w relating pressure and density of cosmological fluid modelling dark energy, *i.e.* $p = w\rho$.
- Parameter estimates of $\boxed{\Omega_\Lambda = 0.63^{+0.18}_{-0.17}}$ and $\boxed{w = -0.77^{+0.35}_{-0.36}}$ obtained.

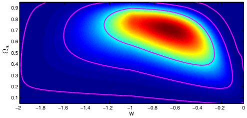

(a) Full likelihood surface

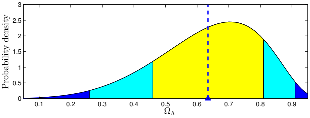

(b) Marginalised distribution for Ω_Λ

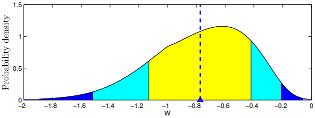

(c) Marginalised distribution for w

Figure: Likelihood for dark energy parameters.

Outline

Cosmic strings

- Symmetry breaking phase transitions in the early Universe $\rightarrow$ topological defects.
- Cosmic strings well-motivated phenomenon that arise when axial or cylindrical symmetry is broken $\rightarrow$ line-like discontinuities in the fabric of the Universe.
- We have not yet observed cosmic strings but we have observed string-like topological defects in other media.

The detection of cosmic strings would open a new window into the physics of the Universe!

Cosmic strings

- Symmetry breaking phase transitions in the early Universe $\rightarrow$ topological defects.
- Cosmic strings well-motivated phenomenon that arise when axial or cylindrical symmetry is broken $\rightarrow$ line-like discontinuities in the fabric of the Universe.
- We have not yet observed cosmic strings but we have observed string-like topological defects in other media.

Figure: Optical microscope photograph of a thin film of freely suspended nematic liquid crystal after a temperature quench. [Credit: Chuang *et al.* (1991).]

The detection of cosmic strings would open a new window into the physics of the Universe!

Cosmic strings

- Symmetry breaking phase transitions in the early Universe $\rightarrow$ topological defects.
- Cosmic strings well-motivated phenomenon that arise when axial or cylindrical symmetry is broken $\rightarrow$ line-like discontinuities in the fabric of the Universe.
- We have not yet observed cosmic strings but we have observed string-like topological defects in other media.

Figure: Optical microscope photograph of a thin film of freely suspended nematic liquid crystal after a temperature quench. [Credit: Chuang *et al.* (1991).]

The detection of cosmic strings would open a new window into the physics of the Universe!

Observational signatures of cosmic strings

Conical Spacetime

- Spacetime about a cosmic string is conical, with a three-dimensional wedge removed (Vilenkin 1981).
- Strings moving transverse to the line of sight induce line-like discontinuities in the CMB (Kaiser & Stebbins 1984).
- The amplitude of the induced contribution scales with the string tension $G\mu$.

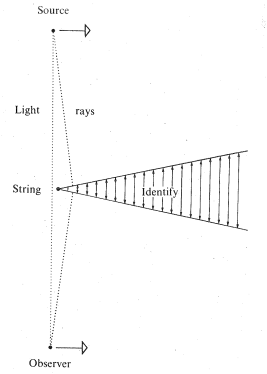

Figure: Spacetime around a cosmic string.
[Credit: Kaiser & Stebbins 1984, DAMTP.]

Observational signatures of cosmic strings

CMB contribution

- Make contact between theory and data using high-resolution simulations.
- Search for a weak string signal s embedded in the CMB c, with observations d given by

$$\underbrace{\boxed{d(\theta,\varphi)}}_{\text{observation}} = \underbrace{\boxed{c(\theta,\varphi)}}_{\text{CMB}} + \underbrace{\boxed{G\mu \cdot s(\theta,\varphi)}}_{\text{strings}} .$$

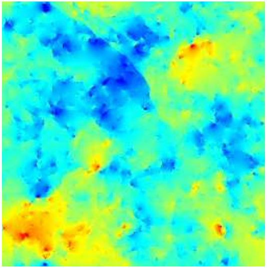

(a) Flat patch (Fraisse *et al.* 2008)

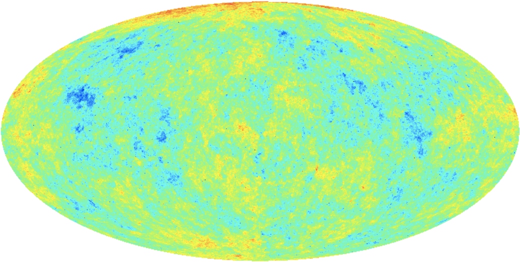

(b) Full-sky (Ringeval *et al.* 2012)

Figure: Cosmic string simulations.

Observational signatures of cosmic strings

CMB contribution

- Make contact between theory and data using high-resolution simulations.
- Search for a weak string signal s embedded in the CMB c, with observations d given by

$$\underbrace{\boxed{d(\theta, \varphi)}}_{\text{observation}} = \underbrace{\boxed{c(\theta, \varphi)}}_{\text{CMB}} + \underbrace{\boxed{G\mu \cdot s(\theta, \varphi)}}_{\text{strings}} .$$

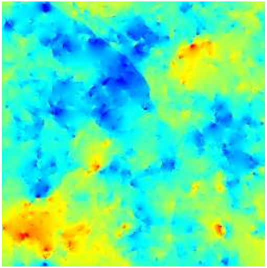

(a) Flat patch (Fraisse *et al.* 2008)

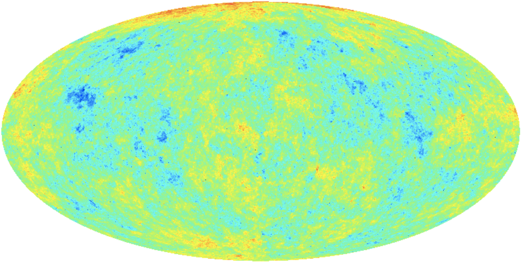

(b) Full-sky (Ringeval *et al.* 2012)

Figure: Cosmic string simulations.

Scale-discretised wavelets on the sphere

Wavelet construction

Exact reconstruction not feasible in practice with continuous wavelets!

- *Exact reconstruction with directional wavelets on the sphere*
  Wiaux, McEwen, Vandergheynst, Blanc (2008)
- Dilation performed in harmonic space [*cf.* McEwen *et al.* (2006), Sanz *et al.* (2006)].

- Scale-discretised wavelet $\Psi^j \in \mathrm{L}^2(\mathbb{S}^2, \mathrm{d}\Omega)$ defined in harmonic space:

$$\Psi^j_{\ell m} \equiv \kappa^j(\ell) s_{\ell m} \, .$$

- Admissible wavelets constructed to satisfy a resolution of the identity:

$$\underbrace{\boxed{|\Phi_{\ell 0}|^2}}_{\text{scaling function}} + \sum_{j=0}^{J} \sum_{m=-\ell}^{\ell} \underbrace{\boxed{|\Psi^j_{\ell m}|^2}}_{\text{wavelet}} = 1 \, , \quad \forall \ell \, .$$

Scale-discretised wavelets on the sphere

Wavelet construction

Exact reconstruction not feasible in practice with continuous wavelets!

- *Exact reconstruction with directional wavelets on the sphere*
  Wiaux, McEwen, Vandergheynst, Blanc (2008)
- Dilation performed in harmonic space [*cf.* McEwen *et al.* (2006), Sanz *et al.* (2006)].

- Scale-discretised wavelet $\Psi^j \in \mathrm{L}^2(\mathbb{S}^2, \mathrm{d}\Omega)$ defined in harmonic space:

$$\Psi^j_{\ell m} \equiv \kappa^j(\ell) s_{\ell m} \, .$$

- Admissible wavelets constructed to satisfy a resolution of the identity:

$$\underbrace{\boxed{|\Phi_{\ell 0}|^2}}_{\text{scaling function}} + \sum_{j=0}^{J} \sum_{m=-\ell}^{\ell} \underbrace{\boxed{|\Psi^j_{\ell m}|^2}}_{\text{wavelet}} = 1 \, , \quad \forall \ell \, .$$

Scale-discretised wavelets on the sphere
Wavelet construction

Exact reconstruction not feasible in practice with continuous wavelets!

- *Exact reconstruction with directional wavelets on the sphere*
  Wiaux, McEwen, Vandergheynst, Blanc (2008)
- Dilation performed in harmonic space [*cf.* McEwen *et al.* (2006), Sanz *et al.* (2006)].

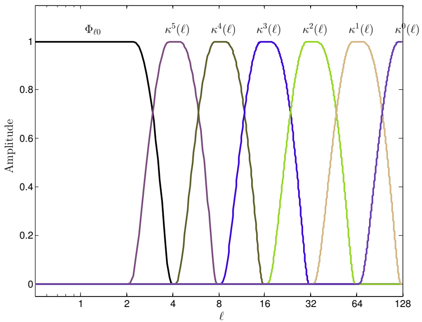

- Scale-discretised wavelet $\Psi^j \in \mathrm{L}^2(\mathbb{S}^2, \mathrm{d}\Omega)$ defined in harmonic space:

$$\Psi^j_{\ell m} \equiv \kappa^j(\ell) s_{\ell m} \ .$$

- Admissible wavelets constructed to satisfy a resolution of the identity:

$$\underbrace{|\Phi_{\ell 0}|^2}_{\text{scaling function}} + \sum_{j=0}^{J} \sum_{m=-\ell}^{\ell} \underbrace{|\Psi^j_{\ell m}|^2}_{\text{wavelet}} = 1 \ , \quad \forall \ell \ .$$

Scale-discretised wavelets on the sphere

Wavelet construction

Exact reconstruction not feasible in practice with continuous wavelets!

- *Exact reconstruction with directional wavelets on the sphere*
  Wiaux, McEwen, Vandergheynst, Blanc (2008)
- Dilation performed in harmonic space [*cf.* McEwen *et al.* (2006), Sanz *et al.* (2006)].

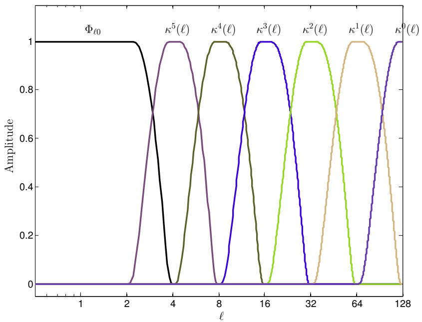

- Scale-discretised wavelet $\Psi^j \in \mathrm{L}^2(\mathbb{S}^2, \mathrm{d}\Omega)$ defined in harmonic space:

$$\Psi^j_{\ell m} \equiv \kappa^j(\ell) s_{\ell m} \ .$$

- Admissible wavelets constructed to satisfy a resolution of the identity:

$$\underbrace{\boxed{|\Phi_{\ell 0}|^2}}_{\text{scaling function}} + \sum_{j=0}^{J} \sum_{m=-\ell}^{\ell} \underbrace{\boxed{|\Psi^j_{\ell m}|^2}}_{\text{wavelet}} = 1 \ , \quad \forall \ell \ .$$

Scale-discretised wavelets on the sphere

Wavelets

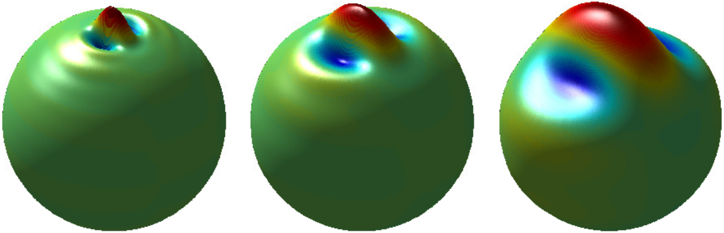

(a) $j = 4$ (b) $j = 3$ (c) $j = 2$

Figure: Scale-discretised wavelets on the sphere.

Scale-discretised wavelets on the sphere

Forward and inverse transform (*i.e.* analysis and synthesis)

- The scale-discretised wavelet transform is given by the usual projection onto each wavelet:

$$\underbrace{\boxed{W^{\Psi^j}(\rho) = \langle f, \mathcal{R}_\rho \Psi^j \rangle}}_{\text{projection}} = \int_{\mathbb{S}^2} \mathrm{d}\Omega(\omega) f(\omega) (\mathcal{R}_\rho \Psi^j)^*(\omega) \ .$$

- The original function may be recovered exactly in practice from the wavelet (and scaling) coefficients:

$$f(\omega) = \underbrace{\boxed{2\pi \int_{\mathbb{S}^2} \mathrm{d}\Omega(\omega') W^{\Phi}(\omega') (\mathcal{R}_{\omega'} L^{\mathrm{d}} \Phi)(\omega)}}_{\text{scaling function contribution}} + \underbrace{\boxed{\sum_{j=0}^{J}}}_{\text{finite sum}} \underbrace{\boxed{\int_{\mathrm{SO}(3)} \mathrm{d}\varrho(\rho) W^{\Psi^j}(\rho) (\mathcal{R}_\rho L^{\mathrm{d}} \Psi^j)(\omega)}}_{\text{wavelet contribution}} \ .$$

Scale-discretised wavelets on the sphere

Forward and inverse transform (*i.e.* analysis and synthesis)

- The scale-discretised wavelet transform is given by the usual projection onto each wavelet:

$$\underbrace{\boxed{W^{\Psi^j}(\rho) = \langle f,\, \mathcal{R}_\rho \Psi^j \rangle}}_{\text{projection}} = \int_{\mathbb{S}^2} \mathrm{d}\Omega(\omega) f(\omega) (\mathcal{R}_\rho \Psi^j)^*(\omega) \,.$$

- The original function may be recovered exactly in practice from the wavelet (and scaling) coefficients:

$$f(\omega) = \underbrace{\boxed{2\pi \int_{\mathbb{S}^2} \mathrm{d}\Omega(\omega') W^{\Phi}(\omega') (\mathcal{R}_{\omega'} L^{\mathrm{d}} \Phi)(\omega)}}_{\text{scaling function contribution}} + \underbrace{\boxed{\sum_{j=0}^{J}}}_{\text{finite sum}} \underbrace{\boxed{\int_{\mathrm{SO}(3)} \mathrm{d}\varrho(\rho) W^{\Psi^j}(\rho) (\mathcal{R}_\rho L^{\mathrm{d}} \Psi^j)(\omega) \,.}}_{\text{wavelet contribution}}$$

Scale-discretised wavelets on the sphere

Exact and efficient computation

- Wavelet analysis can be posed as an inverse Wigner transform on $\mathrm{SO}(3)$:

$$\boxed{W^{\Psi^j}(\rho) = \sum_{\ell=0}^{L-1} \sum_{m=-\ell}^{\ell} \sum_{n=-\ell}^{\ell} \frac{2\ell+1}{8\pi^2} \left(W^{\Psi^j}\right)^{\ell}_{mn} D^{\ell*}_{mn}(\rho) \,,}$$

where $\left(W^{\Psi^j}\right)^{\ell}_{mn} = \frac{8\pi^2}{2\ell+1} f_{\ell m} \Psi^{j*}_{\ell n} \,.$

which can be computed efficiently via a factoring of rotations (Risbo 1996, Wandelt & Gorski 2001, McEwen *et al.* 2007).

- Wavelet synthesis can be posed as an forward Wigner transform on $\mathrm{SO}(3)$:

$$f(\omega) \sim \sum_{j=0}^{J} \int_{\mathrm{SO}(3)} \mathrm{d}\varrho(\rho) W^{\Psi^j}(\rho) (\mathcal{R}_\rho L^{\mathrm{d}} \Psi^j)(\omega) = \sum_{j=0}^{J} \sum_{\ell m n} \frac{2\ell+1}{8\pi^2} \left(W^{\Psi^j}\right)^{\ell}_{mn} \Psi^j_{\ell n} Y_{\ell m}(\omega) \,,$$

where

$$\boxed{\left(W^{\Psi^j}\right)^{\ell}_{mn} = \langle W^{\Psi^j}, D^{\ell*}_{mn} \rangle = \int_{\mathrm{SO}(3)} \mathrm{d}\varrho(\rho) W^{\Psi^j}(\rho) D^{\ell}_{mn}(\rho) \,,}$$

which can be computed efficiently via a factoring of rotations (Risbo 1996, Wiaux, McEwen *et al.* 2008) and exactly by employing the Driscoll & Healy (1994) or McEwen & Wiaux (2011) sampling theorem.

Scale-discretised wavelets on the sphere

Exact and efficient computation

- Wavelet analysis can be posed as an inverse Wigner transform on $\mathrm{SO}(3)$:

$$\boxed{W^{\Psi^j}(\rho) = \sum_{\ell=0}^{L-1} \sum_{m=-\ell}^{\ell} \sum_{n=-\ell}^{\ell} \frac{2\ell+1}{8\pi^2} \left(W^{\Psi^j}\right)^{\ell}_{mn} D^{\ell *}_{mn}(\rho) \, ,}$$ where $$\left(W^{\Psi^j}\right)^{\ell}_{mn} = \frac{8\pi^2}{2\ell+1} f_{\ell m} \Psi^{j*}_{\ell n} \, .$$

which can be computed efficiently via a factoring of rotations (Risbo 1996, Wandelt & Gorski 2001, McEwen *et al.* 2007).

- Wavelet synthesis can be posed as an forward Wigner transform on $\mathrm{SO}(3)$:

$$f(\omega) \sim \sum_{j=0}^{J} \int_{\mathrm{SO}(3)} \mathrm{d}\varrho(\rho) W^{\Psi^j}(\rho) (\mathcal{R}_\rho L^{\mathrm{d}} \Psi^j)(\omega) = \sum_{j=0}^{J} \sum_{\ell m n} \frac{2\ell+1}{8\pi^2} \left(W^{\Psi^j}\right)^{\ell}_{mn} \Psi^j_{\ell n} Y_{\ell m}(\omega) \, ,$$

where

$$\boxed{\left(W^{\Psi^j}\right)^{\ell}_{mn} = \langle W^{\Psi^j}, D^{\ell *}_{mn} \rangle = \int_{\mathrm{SO}(3)} \mathrm{d}\varrho(\rho) W^{\Psi^j}(\rho) D^{\ell}_{mn}(\rho) \, ,}$$

which can be computed efficiently via a factoring of rotations (Risbo 1996, Wiaux, McEwen *et al.* 2008) and exactly by employing the Driscoll & Healy (1994) or McEwen & Wiaux (2011) sampling theorem.

Scale-discretised wavelets on the sphere

Exact and efficient computation

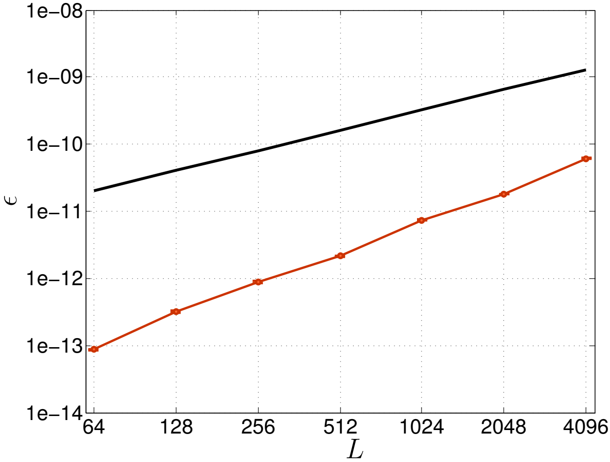

Figure: Numerical accuracy.

Scale-discretised wavelets on the sphere

Exact and efficient computation

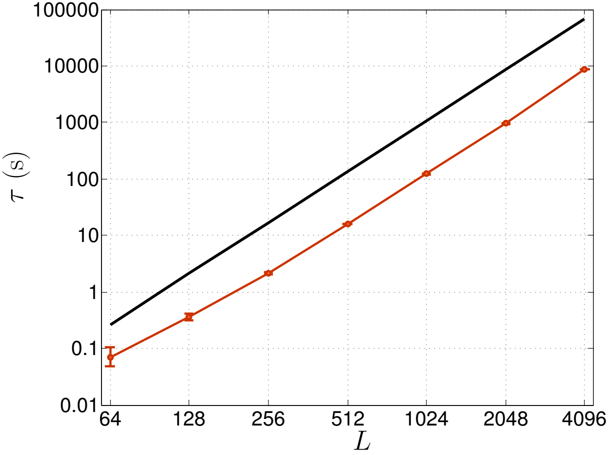

Figure: Computation time.

Scale-discretised wavelets on the sphere

Codes

S2DW code

`http://www.s2dw.org`

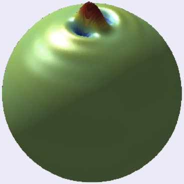

Exact reconstruction with directional wavelets on the sphere
Wiaux, McEwen, Vandergheynst, Blanc (2008)

- Fortran
- Parallelised
- Supports directional and steerable wavelets

S2LET code

`http://www.s2let.org`

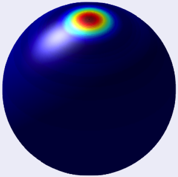

S2LET: A code to perform fast wavelet analysis on the sphere
Leistedt, McEwen, Vandergheynst, Wiaux (2012)

- C, Matlab, IDL, Java
- Supports only axisymmetric wavelets at present
- Future extensions planned (directional and steerable wavelets, faster algos, spin wavelets)

Scale-discretised wavelets on the sphere

Illustration

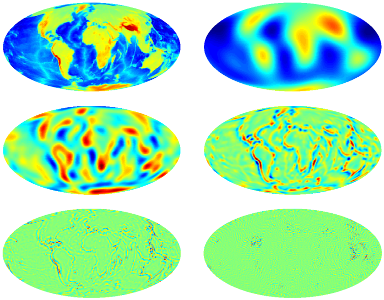

(a) Undecimated

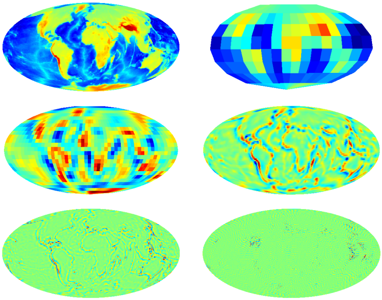

(b) Multi-resolution

Figure: Scale-discretised wavelet transform of a topography map of the Earth.

Motivation for using wavelets to detect cosmic strings

- Denote the wavelet coefficients of the data d by

$$\boxed{W^{d}_{j\rho} = \langle d,\ \Psi_{j\rho} \rangle}$$

for scale $j \in \mathbb{Z}^{+}$ and position $\rho \in \mathrm{SO}(3)$.

- Consider an even azimuthal band-limit $N = 4$ to yield wavelet with odd azimuthal symmetry.

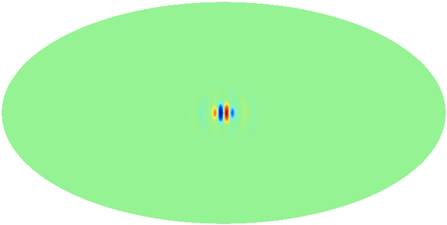

Figure: Example wavelet matched to the expected string contribution.

Motivation for using wavelets to detect cosmic strings

- Wavelet transform yields a sparse representation of the string signal → hope to effectively separate the CMB and string signal in wavelet space.

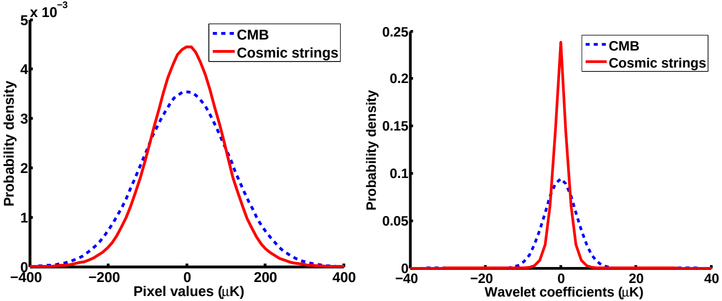

Figure: Distribution of CMB and string signal in pixel (left) and wavelet space (right).

Learning the statistics of the CMB and string signals in wavelet space

- Wavelet-Bayesian approach to estimate the string tension and map:

$$\underbrace{\boxed{d(\theta,\varphi)}}_{\text{observation}} = \underbrace{\boxed{c(\theta,\varphi)}}_{\text{CMB}} + \underbrace{\boxed{G\mu \cdot s(\theta,\varphi)}}_{\text{strings}} .$$

- Need to determine statistical description of the CMB and string signals in wavelet space.

- Calculate analytically the probability distribution of the CMB in wavelet space.

- Fit a generalised Gaussian distribution (GGD) for the wavelet coefficients of a string training map (*cf.* Wiaux *et al.* 2009):

$$\mathrm{P}_j^s(W_{j\rho}^s \,|\, G\mu) = \frac{\upsilon_j}{2G\mu\nu_j\Gamma(\upsilon_j{}^{-1})}\,\mathrm{e}^{\left(-\left|\frac{W_{j\rho}^s}{G\mu\nu_j}\right|^{\upsilon_j}\right)} ,$$

with scale parameter ν_j and shape parameter υ_j.

Learning the statistics of the CMB and string signals in wavelet space

- Wavelet-Bayesian approach to estimate the string tension and map:

$$\underbrace{\boxed{d(\theta,\varphi)}}_{\text{observation}} = \underbrace{\boxed{c(\theta,\varphi)}}_{\text{CMB}} + \underbrace{\boxed{G\mu \cdot s(\theta,\varphi)}}_{\text{strings}} .$$

- Need to determine statistical description of the CMB and string signals in wavelet space.
- Calculate analytically the probability distribution of the CMB in wavelet space.
- Fit a generalised Gaussian distribution (GGD) for the wavelet coefficients of a string training map (*cf.* Wiaux *et al.* 2009):

$$\mathrm{P}_j^s(W_{j\rho}^s \,|\, G\mu) = \frac{\upsilon_j}{2G\mu\nu_j\Gamma(\upsilon_j{}^{-1})}\, \mathrm{e}^{\left(-\left|\frac{W_{j\rho}^s}{G\mu\nu_j}\right|^{\upsilon_j}\right)} ,$$

with scale parameter ν_j and shape parameter υ_j.

Learning the statistics of the CMB and string signals in wavelet space

- Wavelet-Bayesian approach to estimate the string tension and map:

$$\underbrace{\boxed{d(\theta,\varphi)}}_{\text{observation}} = \underbrace{\boxed{c(\theta,\varphi)}}_{\text{CMB}} + \underbrace{\boxed{G\mu \cdot s(\theta,\varphi)}}_{\text{strings}} .$$

- Need to determine statistical description of the CMB and string signals in wavelet space.
- Calculate analytically the probability distribution of the CMB in wavelet space.
- Fit a generalised Gaussian distribution (GGD) for the wavelet coefficients of a string training map (*cf.* Wiaux *et al.* 2009):

$$\mathrm{P}_j^s(W_{j\rho}^s \,|\, G\mu) = \frac{\upsilon_j}{2G\mu\nu_j\Gamma(\upsilon_j{}^{-1})} \, \mathrm{e}^{\left(-\left|\frac{W_{j\rho}^s}{G\mu\nu_j}\right|^{\upsilon_j}\right)} ,$$

with scale parameter ν_j and shape parameter υ_j.

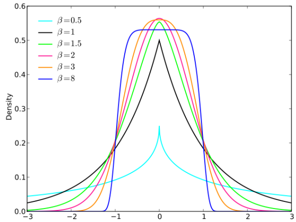

Figure: GGD

Learning the statistics of the CMB and string signals in wavelet space

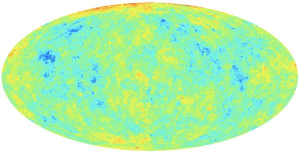

(a) String training map (b) String testing map

Figure: Cosmic string simulations.

- Distributions in close agreement.

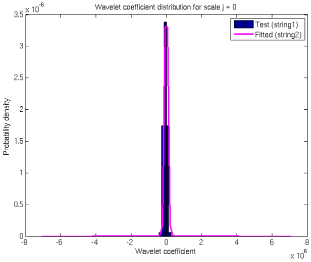

Figure: Distributions for wavelet scale $j = 0$.

Learning the statistics of the CMB and string signals in wavelet space

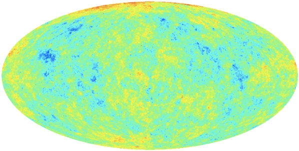

(a) String training map

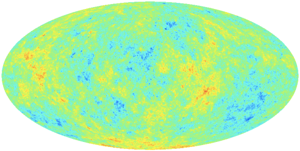

(b) String testing map

Figure: Cosmic string simulations.

- Distributions in close agreement.

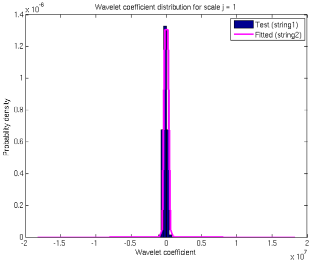

Figure: Distributions for wavelet scale $j = 1$.

Learning the statistics of the CMB and string signals in wavelet space

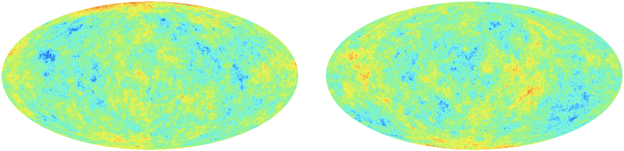

(a) String training map (b) String testing map

Figure: Cosmic string simulations.

- Distributions in close agreement.

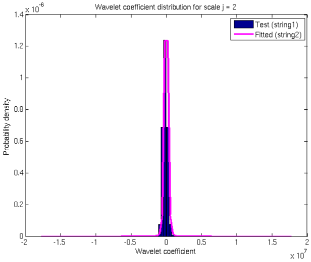

Figure: Distributions for wavelet scale $j = 2$.

Learning the statistics of the CMB and string signals in wavelet space

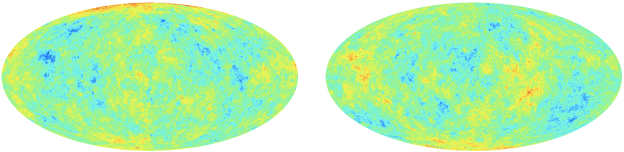

(a) String training map (b) String testing map

Figure: Cosmic string simulations.

- Distributions in close agreement.

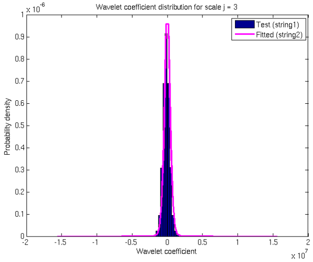

Figure: Distributions for wavelet scale $j = 3$.

Learning the statistics of the CMB and string signals in wavelet space

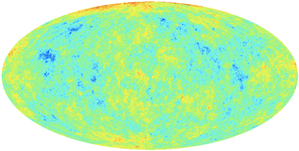

(a) String training map (b) String testing map

Figure: Cosmic string simulations.

- Distributions in close agreement.
- Accurately characterised statistics of string signals in wavelet space.

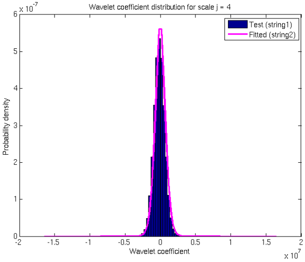

Figure: Distributions for wavelet scale $j = 4$.

Spherical wavelet-Bayesian string tension estimation

- Perform Bayesian string tension estimation in wavelet space.
- For each wavelet coefficient the likelihood is given by

$$\mathrm{P}(W^d_{j\rho} \,|\, G\mu) = \mathrm{P}(W^s_{j\rho} + W^c_{j\rho} \,|\, G\mu) = \int_{\mathbb{R}} \mathrm{d}W^s_{j\rho} \, \mathrm{P}^c_j(W^d_{j\rho} - W^s_{j\rho}) \, \mathrm{P}^s_j(W^s_{j\rho} \,|\, G\mu) \, .$$

- The overall likelihood of the data is given by

$$\mathrm{P}(W^d \,|\, G\mu) = \prod_{j,\rho} \mathrm{P}(W^d_{j\rho} \,|\, G\mu) \, ,$$

where we have assumed independence for numerical tractability.

Spherical wavelet-Bayesian string tension estimation

- Perform Bayesian string tension estimation in wavelet space.
- For each wavelet coefficient the likelihood is given by

$$\boxed{\mathrm{P}(W^d_{j\rho} \mid G\mu) = \mathrm{P}(W^s_{j\rho} + W^c_{j\rho} \mid G\mu) = \int_{\mathbb{R}} \mathrm{d}W^s_{j\rho}\, \mathrm{P}^c_j(W^d_{j\rho} - W^s_{j\rho})\, \mathrm{P}^s_j(W^s_{j\rho} \mid G\mu)\ .}$$

- The overall likelihood of the data is given by

$$\boxed{\mathrm{P}(W^d \mid G\mu) = \prod_{j,\rho} \mathrm{P}(W^d_{j\rho} \mid G\mu)\ ,}$$

where we have assumed independence for numerical tractability.

Spherical wavelet-Bayesian string tension estimation

- Perform Bayesian string tension estimation in wavelet space.
- For each wavelet coefficient the likelihood is given by

$$\boxed{\mathrm{P}(W^d_{j\rho} \,|\, G\mu) = \mathrm{P}(W^s_{j\rho} + W^c_{j\rho} \,|\, G\mu) = \int_{\mathbb{R}} \mathrm{d}W^s_{j\rho}\, \mathrm{P}^c_j(W^d_{j\rho} - W^s_{j\rho})\, \mathrm{P}^s_j(W^s_{j\rho} \,|\, G\mu)\ .}$$

- The overall likelihood of the data is given by

$$\boxed{\mathrm{P}(W^d \,|\, G\mu) = \prod_{j,\rho} \mathrm{P}(W^d_{j\rho} \,|\, G\mu)\ ,}$$

where we have assumed independence for numerical tractability.

Spherical wavelet-Bayesian string tension estimation

- Compute the string tension posterior $\mathrm{P}(G\mu \mid W^d)$ by Bayes theorem:

$$\boxed{\mathrm{P}(G\mu \mid W^d) = \frac{\mathrm{P}(W^d \mid G\mu)\,\mathrm{P}(G\mu)}{\mathrm{P}(W^d)} \propto \mathrm{P}(W^d \mid G\mu)\,\mathrm{P}(G\mu)\,.}$$

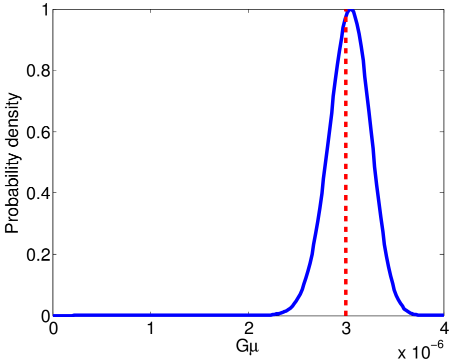

Figure: Posterior distribution of the string tension (true $G\mu = 3 \times 10^{-6}$).

Spherical wavelet-Bayesian string tension estimation

- Compute the string tension posterior $\mathrm{P}(G\mu \mid W^d)$ by Bayes theorem:

$$\boxed{\mathrm{P}(G\mu \mid W^d) = \frac{\mathrm{P}(W^d \mid G\mu)\,\mathrm{P}(G\mu)}{\mathrm{P}(W^d)} \propto \mathrm{P}(W^d \mid G\mu)\,\mathrm{P}(G\mu)\ .}$$

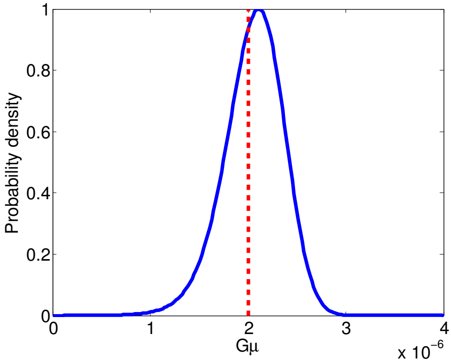

Figure: Posterior distribution of the string tension (true $G\mu = 2 \times 10^{-6}$).

Spherical wavelet-Bayesian string tension estimation

- Compute the string tension posterior $\mathrm{P}(G\mu \mid W^d)$ by Bayes theorem:

$$\boxed{\mathrm{P}(G\mu \mid W^d) = \frac{\mathrm{P}(W^d \mid G\mu)\,\mathrm{P}(G\mu)}{\mathrm{P}(W^d)} \propto \mathrm{P}(W^d \mid G\mu)\,\mathrm{P}(G\mu)\ .}$$

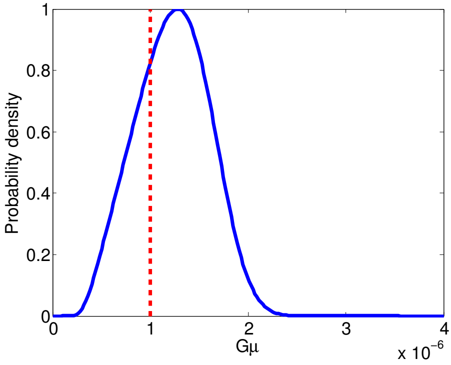

Figure: Posterior distribution of the string tension (true $G\mu = 1 \times 10^{-6}$).

Bayesian evidence for strings

- Compute Bayesian evidences to compare the string model M^s to the alternative model M^c that the observed data is comprised of just a CMB contribution.
- The Bayesian evidence of the string model is given by

$$E^s = \mathrm{P}(W^d \mid \mathrm{M}^s) = \int_{\mathbb{R}} \mathrm{d}(G\mu)\, \mathrm{P}(W^d \mid G\mu)\, \mathrm{P}(G\mu) \; .$$

- The Bayesian evidence of the CMB model is given by

$$E^c = \mathrm{P}(W^d \mid \mathrm{M}^c) = \prod_{j,\rho} \mathrm{P}_j^c(W_{j\rho}^d) \; .$$

- Compute the Bayes factor to determine the preferred model:

$$\Delta \ln E = \ln(E^s / E^c) \; .$$

Bayesian evidence for strings

- Compute Bayesian evidences to compare the string model M^s to the alternative model M^c that the observed data is comprised of just a CMB contribution.
- The Bayesian evidence of the string model is given by

$$\boxed{E^s = \mathrm{P}(W^d \,|\, \mathrm{M}^s) = \int_{\mathbb{R}} \mathrm{d}(G\mu)\, \mathrm{P}(W^d \,|\, G\mu)\, \mathrm{P}(G\mu) \,.}$$

- The Bayesian evidence of the CMB model is given by

$$\boxed{E^c = \mathrm{P}(W^d \,|\, \mathrm{M}^c) = \prod_{j,\rho} \mathrm{P}^c_j(W^d_{j\rho}) \,.}$$

- Compute the Bayes factor to determine the preferred model:

$$\boxed{\Delta \ln E = \ln(E^s / E^c) \,.}$$

Bayesian evidence for strings

- Compute Bayesian evidences to compare the string model M^s to the alternative model M^c that the observed data is comprised of just a CMB contribution.

- The Bayesian evidence of the string model is given by

$$E^s = \mathrm{P}(W^d \mid \mathrm{M}^s) = \int_{\mathbb{R}} \mathrm{d}(G\mu)\, \mathrm{P}(W^d \mid G\mu)\, \mathrm{P}(G\mu) \, .$$

- The Bayesian evidence of the CMB model is given by

$$E^c = \mathrm{P}(W^d \mid \mathrm{M}^c) = \prod_{j,\rho} \mathrm{P}^c_j(W^d_{j\rho}) \, .$$

- Compute the Bayes factor to determine the preferred model:

$$\Delta \ln E = \ln(E^s / E^c) \, .$$

Bayesian evidence for strings

- Compute Bayesian evidences to compare the string model M^s to the alternative model M^c that the observed data is comprised of just a CMB contribution.
- The Bayesian evidence of the string model is given by

$$\boxed{E^s = \mathrm{P}(W^d \mid \mathrm{M}^s) = \int_{\mathbb{R}} \mathrm{d}(G\mu)\, \mathrm{P}(W^d \mid G\mu)\, \mathrm{P}(G\mu)\ .}$$

- The Bayesian evidence of the CMB model is given by

$$\boxed{E^c = \mathrm{P}(W^d \mid \mathrm{M}^c) = \prod_{j,\rho} \mathrm{P}_j^c(W_{j\rho}^d)\ .}$$

- Compute the Bayes factor to determine the preferred model:

$$\boxed{\Delta \ln E = \ln(E^s / E^c)\ .}$$

Table: Tension estimates and log-evidence differences for simulations.

$G\mu/10^{-6}$	0.7	0.8	0.9	1.0	2.0	3.0
$\widehat{G\mu}/10^{-6}$	1.1	1.2	1.2	1.3	2.1	3.1
$\Delta\ln E$	-1.3	-1.1	-0.9	-0.7	5.5	29

Recovering string maps

- Inference of the wavelet coefficients of the underlying string map encoded in posterior probability distribution $\mathrm{P}(W^s_{j\rho} \mid W^d)$.
- Estimate the wavelet coefficients of the string map from the mean of the posterior distribution:

$$\boxed{\overline{W}^s_{j\rho} = \int_{\mathbb{R}} \mathrm{d}W^s_{j\rho} \, W^s_{j\rho} \, \mathrm{P}(W^s_{j\rho} \mid W^d)}$$

- Recover the string map from its wavelets (possible since the scale-discretised wavelet transform on the sphere supports exact reconstruction).
- Work in progress...

Recovering string maps

- Inference of the wavelet coefficients of the underlying string map encoded in posterior probability distribution $\mathrm{P}(W^{s}_{j\rho} \mid W^{d})$.
- Estimate the wavelet coefficients of the string map from the mean of the posterior distribution:

$$\boxed{\overline{W}^{s}_{j\rho} = \int_{\mathbb{R}} \mathrm{d}W^{s}_{j\rho} \, W^{s}_{j\rho} \, \mathrm{P}(W^{s}_{j\rho} \mid W^{d})}$$

- Recover the string map from its wavelets (possible since the scale-discretised wavelet transform on the sphere supports exact reconstruction).
- Work in progress. . .

Outline

1. Dark energy
   - ISW effect
   - Continuous wavelets on the sphere
   - Detecting dark energy
2. Cosmic strings
   - String physics
   - Scale-discretised wavelets on the sphere
   - String estimation
3. Radio interferometry
   - Interferometric imaging
   - Compressive sensing
   - Imaging with CS
4. Large-scale structure
   - Wavelets on ball
   - Cosmic voids

Next-generation of radio interferometry rapidly approaching

- Square Kilometre Array (SKA) construction scheduled to begin in 2018.
- Many other pathfinder telescopes under construction, *e.g.* LOFAR, ASKAP, MeerKAT, MWA.
- New modelling and imaging techniques required to ensure the next-generation of interferometric telescopes reach their full potential.

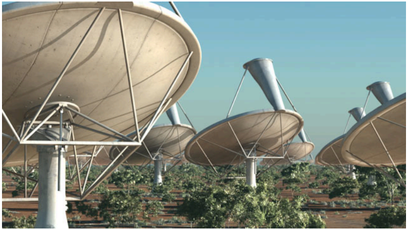

Figure: Artist impression of SKA dishes. [Credit: SKA Organisation]

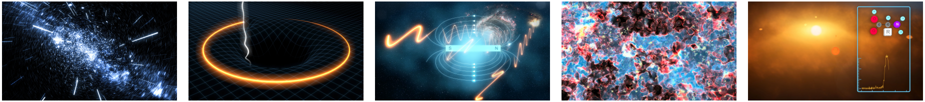

(a) Dark-energy (b) GR (c) Cosmic magnetism (d) **Epoch of reionization** (e) Exoplanets

Figure: SKA science goals. [Credit: SKA Organisation]

Next-generation of radio interferometry rapidly approaching

- Square Kilometre Array (SKA) construction scheduled to begin in 2018.
- Many other pathfinder telescopes under construction, *e.g.* LOFAR, ASKAP, MeerKAT, MWA.
- New modelling and imaging techniques required to ensure the next-generation of interferometric telescopes reach their full potential.

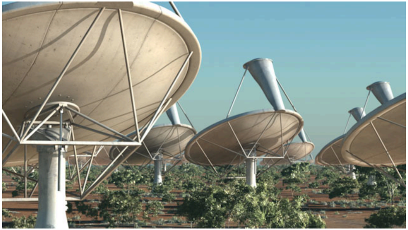

Figure: Artist impression of SKA dishes. [Credit: SKA Organisation]

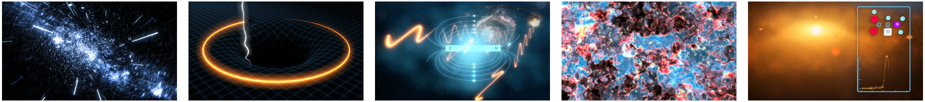

(a) Dark-energy (b) GR (c) Cosmic magnetism (d) **Epoch of reionization** (e) Exoplanets

Figure: SKA science goals. [Credit: SKA Organisation]

Radio interferometry

- The complex visibility measured by an interferometer is given by

$$\boxed{y(\boldsymbol{u}, w) = \int_{D^2} A(\boldsymbol{l})\, x(\boldsymbol{l})\, C(\|\boldsymbol{l}\|_2)\, \mathrm{e}^{-\mathrm{i}2\pi \boldsymbol{u}\cdot\boldsymbol{l}}\, \frac{\mathrm{d}^2\boldsymbol{l}}{n(\boldsymbol{l})}},$$

visibilities

where the w-modulation $C(\|\boldsymbol{l}\|_2)$ is given by

$$\boxed{C(\|\boldsymbol{l}\|_2) \equiv \mathrm{e}^{\mathrm{i}2\pi w\left(1-\sqrt{1-\|\boldsymbol{l}\|^2}\right)}}.$$

w-modulation

- Various assumptions are often made regarding the size of the field-of-view (FoV):
  - Small-field with $\boxed{\|\boldsymbol{l}\|^2 w \ll 1}$ $\Rightarrow$ $\boxed{C(\|\boldsymbol{l}\|_2) \simeq 1}$
  - Small-field with $\boxed{\|\boldsymbol{l}\|^4 w \ll 1}$ $\Rightarrow$ $\boxed{C(\|\boldsymbol{l}\|_2) \simeq \mathrm{e}^{\mathrm{i}\pi w\|\boldsymbol{l}\|^2}}$
  - Wide-field $\Rightarrow$ $\boxed{C(\|\boldsymbol{l}\|_2) = \mathrm{e}^{\mathrm{i}2\pi w\left(1-\sqrt{1-\|\boldsymbol{l}\|^2}\right)}}$

Radio interferometry

- The complex visibility measured by an interferometer is given by

$$\boxed{y(\boldsymbol{u}, w) = \int_{D^2} A(\boldsymbol{l})\, x(\boldsymbol{l})\, C(\|\boldsymbol{l}\|_2)\, \mathrm{e}^{-\mathrm{i}2\pi \boldsymbol{u}\cdot\boldsymbol{l}}\, \frac{\mathrm{d}^2\boldsymbol{l}}{n(\boldsymbol{l})}},$$

visibilities

where the w-modulation $C(\|\boldsymbol{l}\|_2)$ is given by

$$\boxed{C(\|\boldsymbol{l}\|_2) \equiv \mathrm{e}^{\mathrm{i}2\pi w\left(1-\sqrt{1-\|\boldsymbol{l}\|^2}\right)}}.$$

w-modulation

- Various assumptions are often made regarding the size of the field-of-view (FoV):
  - Small-field with $\boxed{\|\boldsymbol{l}\|^2\, w \ll 1}$ $\Rightarrow$ $\boxed{C(\|\boldsymbol{l}\|_2) \simeq 1}$
  - Small-field with $\boxed{\|\boldsymbol{l}\|^4\, w \ll 1}$ $\Rightarrow$ $\boxed{C(\|\boldsymbol{l}\|_2) \simeq \mathrm{e}^{\mathrm{i}\pi w \|\boldsymbol{l}\|^2}}$
  - Wide-field $\Rightarrow$ $\boxed{C(\|\boldsymbol{l}\|_2) = \mathrm{e}^{\mathrm{i}2\pi w\left(1-\sqrt{1-\|\boldsymbol{l}\|^2}\right)}}$

Radio interferometry

- The complex visibility measured by an interferometer is given by

$$\boxed{y(\boldsymbol{u}, w) = \int_{D^2} A(\boldsymbol{l})\, x(\boldsymbol{l})\, C(\|\boldsymbol{l}\|_2)\, \mathrm{e}^{-\mathrm{i}2\pi \boldsymbol{u}\cdot\boldsymbol{l}}\, \frac{\mathrm{d}^2\boldsymbol{l}}{n(\boldsymbol{l})}},$$

visibilities

where the w-modulation $C(\|\boldsymbol{l}\|_2)$ is given by

$$\boxed{C(\|\boldsymbol{l}\|_2) \equiv \mathrm{e}^{\mathrm{i}2\pi w\left(1-\sqrt{1-\|\boldsymbol{l}\|^2}\right)}}.$$

w-modulation

- Various assumptions are often made regarding the size of the field-of-view (FoV):
  - Small-field with $\boxed{\|\boldsymbol{l}\|^2\, w \ll 1}$ $\Rightarrow$ $\boxed{C(\|\boldsymbol{l}\|_2) \simeq 1}$
  - Small-field with $\boxed{\|\boldsymbol{l}\|^4\, w \ll 1}$ $\Rightarrow$ $\boxed{C(\|\boldsymbol{l}\|_2) \simeq \mathrm{e}^{\mathrm{i}\pi w \|\boldsymbol{l}\|^2}}$
  - Wide-field $\Rightarrow$ $\boxed{C(\|\boldsymbol{l}\|_2) = \mathrm{e}^{\mathrm{i}2\pi w\left(1-\sqrt{1-\|\boldsymbol{l}\|^2}\right)}}$

Radio interferometric inverse problem

- Consider the ill-posed inverse problem of radio interferometric imaging:

$$\boxed{\boldsymbol{y} = \Phi \boldsymbol{x} + \boldsymbol{n}},$$

where $\boldsymbol{y}$ are the measured visibilities, Φ is the linear measurement operator, $\boldsymbol{x}$ is the underlying image and $\boldsymbol{n}$ is instrumental noise.

- Measurement operator $\boxed{\Phi = \mathbf{M}\,\mathbf{F}\,\mathbf{C}\,\mathbf{A}}$ may incorporate:
  - primary beam $\mathbf{A}$ of the telescope;
  - w-modulation modulation $\mathbf{C}$;
  - Fourier transform $\mathbf{F}$;
  - masking $\mathbf{M}$ which encodes the incomplete measurements taken by the interferometer.

Radio interferometric inverse problem

- Consider the ill-posed inverse problem of radio interferometric imaging:

$$\boxed{\boldsymbol{y} = \Phi \boldsymbol{x} + \boldsymbol{n}},$$

  where $\boldsymbol{y}$ are the measured visibilities, Φ is the linear measurement operator, $\boldsymbol{x}$ is the underlying image and $\boldsymbol{n}$ is instrumental noise.

- Measurement operator $\boxed{\Phi = \mathbf{M}\,\mathbf{F}\,\mathbf{C}\,\mathbf{A}}$ may incorporate:
  - primary beam $\mathbf{A}$ of the telescope;
  - w-modulation modulation $\mathbf{C}$;
  - Fourier transform $\mathbf{F}$;
  - masking $\mathbf{M}$ which encodes the incomplete measurements taken by the interferometer.

Radio interferometric inverse problem

- Consider the ill-posed inverse problem of radio interferometric imaging:

$$\boxed{\boldsymbol{y} = \Phi \boldsymbol{x} + \boldsymbol{n}} \,,$$

where $\boldsymbol{y}$ are the measured visibilities, Φ is the linear measurement operator, $\boldsymbol{x}$ is the underlying image and $\boldsymbol{n}$ is instrumental noise.

- Measurement operator $\boxed{\Phi = \mathbf{M}\,\mathbf{F}\,\mathbf{C}\,\mathbf{A}}$ may incorporate:
  - primary beam $\mathbf{A}$ of the telescope;
  - w-modulation modulation $\mathbf{C}$;
  - Fourier transform $\mathbf{F}$;
  - masking $\mathbf{M}$ which encodes the incomplete measurements taken by the interferometer.

Interferometric imaging: recover an image from noisy and incomplete Fourier measurements.

Compressive sensing

"Nothing short of revolutionary."

– National Science Foundation

- Developed by Emmanuel Candes and David Donoho (and others).

(a) Emmanuel Candes

(b) David Donoho

Compressive sensing

- Next evolution of wavelet analysis $\rightarrow$ wavelets are a key ingredient.
- The mystery of JPEG compression (discrete cosine transform; wavelet transform).
- Move compression to the acquisition stage $\rightarrow$ compressive sensing.
- Acquisition versus imaging.

Compressive sensing

- Next evolution of wavelet analysis $\rightarrow$ wavelets are a key ingredient.
- The mystery of JPEG compression (discrete cosine transform; wavelet transform).
- Move compression to the acquisition stage $\rightarrow$ compressive sensing.
- Acquisition versus imaging.

Compressive sensing

- Next evolution of wavelet analysis → wavelets are a key ingredient.
- The mystery of JPEG compression (discrete cosine transform; wavelet transform).
- Move compression to the acquisition stage → compressive sensing.
- Acquisition versus imaging.

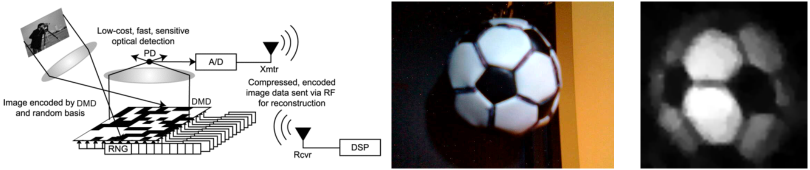

(a) Architecture (b) Scene (c) Recov. (20% meas.)

Figure: Single pixel camera

Compressive sensing

- Next evolution of wavelet analysis → wavelets are a key ingredient.
- The mystery of JPEG compression (discrete cosine transform; wavelet transform).
- Move compression to the acquisition stage → compressive sensing.
- Acquisition versus imaging.

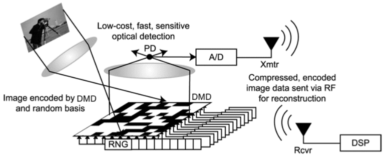

(a) Architecture

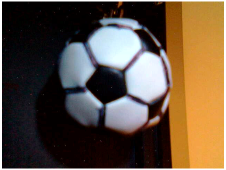

(b) Scene

(c) Recov. (20% meas.)

Figure: Single pixel camera

An introduction to compressive sensing

Operator description

- Linear operator (linear algebra) representation of signal decomposition:

$$x(t) = \sum_i \alpha_i \Psi_i(t) \quad \rightarrow \quad \boldsymbol{x} = \sum_i \Psi_i \alpha_i = \begin{pmatrix} | \\ \Psi_0 \\ | \end{pmatrix} \alpha_0 + \begin{pmatrix} | \\ \Psi_1 \\ | \end{pmatrix} \alpha_1 + \cdots \quad \rightarrow \quad \boxed{\boldsymbol{x} = \Psi \boldsymbol{\alpha}}$$

- Linear operator (linear algebra) representation of measurement:

$$y_i = \langle x, \Phi_j \rangle \quad \rightarrow \quad \boldsymbol{y} = \begin{pmatrix} - \Phi_0 - \\ - \Phi_1 - \\ \vdots \end{pmatrix} \boldsymbol{x} \quad \rightarrow \quad \boxed{\boldsymbol{y} = \Phi \boldsymbol{x}}$$

- Putting it together: $\boxed{\boldsymbol{y} = \Phi \boldsymbol{x} = \Phi \Psi \boldsymbol{\alpha}}$

An introduction to compressive sensing

Operator description

- Linear operator (linear algebra) representation of signal decomposition:

$$x(t) = \sum_i \alpha_i \Psi_i(t) \quad \rightarrow \quad \boldsymbol{x} = \sum_i \Psi_i \alpha_i = \begin{pmatrix} | \\ \Psi_0 \\ | \end{pmatrix} \alpha_0 + \begin{pmatrix} | \\ \Psi_1 \\ | \end{pmatrix} \alpha_1 + \cdots \quad \rightarrow \quad \boxed{\boldsymbol{x} = \Psi \boldsymbol{\alpha}}$$

- Linear operator (linear algebra) representation of measurement:

$$y_i = \langle x, \Phi_j \rangle \quad \rightarrow \quad \boldsymbol{y} = \begin{pmatrix} - \; \Phi_0 \; - \\ - \; \Phi_1 \; - \\ \vdots \end{pmatrix} \boldsymbol{x} \quad \rightarrow \quad \boxed{\boldsymbol{y} = \Phi \boldsymbol{x}}$$

- Putting it together: $\boxed{\boldsymbol{y} = \Phi \boldsymbol{x} = \Phi \Psi \boldsymbol{\alpha}}$

An introduction to compressive sensing

Operator description

- Linear operator (linear algebra) representation of signal decomposition:

$$x(t) = \sum_i \alpha_i \Psi_i(t) \quad \rightarrow \quad \boldsymbol{x} = \sum_i \Psi_i \alpha_i = \begin{pmatrix} | \\ \Psi_0 \\ | \end{pmatrix} \alpha_0 + \begin{pmatrix} | \\ \Psi_1 \\ | \end{pmatrix} \alpha_1 + \cdots \quad \rightarrow \quad \boxed{\boldsymbol{x} = \Psi \boldsymbol{\alpha}}$$

- Linear operator (linear algebra) representation of measurement:

$$y_i = \langle x, \Phi_j \rangle \quad \rightarrow \quad \boldsymbol{y} = \begin{pmatrix} - \ \Phi_0 \ - \\ - \ \Phi_1 \ - \\ \vdots \end{pmatrix} \boldsymbol{x} \quad \rightarrow \quad \boxed{\boldsymbol{y} = \Phi \boldsymbol{x}}$$

- Putting it together: $\boxed{\boldsymbol{y} = \Phi \boldsymbol{x} = \Phi \Psi \boldsymbol{\alpha}}$

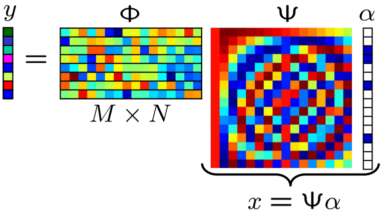

An introduction to compressive sensing

Promoting sparsity via ℓ_1 minimisation

- Ill-posed inverse problem:

$$\boxed{\boldsymbol{y} = \Phi \boldsymbol{x} + \boldsymbol{n} = \Phi \Psi \boldsymbol{\alpha} + \boldsymbol{n}}\,.$$

- Recall norms given by:

$$\|\alpha\|_0 = \text{no. non-zero elements} \qquad \|\alpha\|_1 = \sum_i |\alpha_i| \qquad \|\alpha\|_2 = \Big(\sum_i |\alpha_i|^2\Big)^{1/2}$$

- Solve by imposing a regularising prior that the signal to be recovered is sparse in Ψ, *i.e.* solve the following ℓ_0 optimisation problem:

$$\boxed{\boldsymbol{\alpha}^\star = \arg\min_{\boldsymbol{\alpha}} \|\alpha\|_0 \ \text{such that} \ \|\boldsymbol{y} - \Phi\Psi\boldsymbol{\alpha}\|_2 \leq \epsilon}\,,$$

where the signal is synthesising by $\boldsymbol{x}^\star = \Psi\boldsymbol{\alpha}^\star$.

- Solving this problem is difficult (combinatorial).
- Instead, solve the ℓ_1 optimisation problem (convex):

$$\boxed{\boldsymbol{\alpha}^\star = \arg\min_{\boldsymbol{\alpha}} \|\alpha\|_1 \ \text{such that} \ \|\boldsymbol{y} - \Phi\Psi\boldsymbol{\alpha}\|_2 \leq \epsilon}\,.$$

An introduction to compressive sensing

Promoting sparsity via ℓ_1 minimisation

- Ill-posed inverse problem:

$$\boxed{\boldsymbol{y} = \Phi \boldsymbol{x} + \boldsymbol{n} = \Phi \Psi \boldsymbol{\alpha} + \boldsymbol{n}}\,.$$

- Recall norms given by:

$$\|\alpha\|_0 = \text{no. non-zero elements} \qquad \|\alpha\|_1 = \sum_i |\alpha_i| \qquad \|\alpha\|_2 = \Big(\sum_i |\alpha_i|^2\Big)^{1/2}$$

- Solve by imposing a regularising prior that the signal to be recovered is sparse in Ψ, *i.e.* solve the following ℓ_0 optimisation problem:

$$\boxed{\boldsymbol{\alpha}^\star = \arg\min_{\boldsymbol{\alpha}} \|\alpha\|_0 \;\text{ such that }\; \|\boldsymbol{y} - \Phi\Psi\boldsymbol{\alpha}\|_2 \leq \epsilon}\,,$$

where the signal is synthesising by $\boldsymbol{x}^\star = \Psi \boldsymbol{\alpha}^\star$.

- Solving this problem is difficult (combinatorial).
- Instead, solve the ℓ_1 optimisation problem (convex):

$$\boxed{\boldsymbol{\alpha}^\star = \arg\min_{\boldsymbol{\alpha}} \|\alpha\|_1 \;\text{ such that }\; \|\boldsymbol{y} - \Phi\Psi\boldsymbol{\alpha}\|_2 \leq \epsilon}\,.$$

An introduction to compressive sensing

Promoting sparsity via ℓ_1 minimisation

- Ill-posed inverse problem:

$$\boxed{\boldsymbol{y} = \Phi \boldsymbol{x} + \boldsymbol{n} = \Phi \Psi \boldsymbol{\alpha} + \boldsymbol{n}} \, .$$

- Recall norms given by:

$$\|\alpha\|_0 = \text{no. non-zero elements} \qquad \|\alpha\|_1 = \sum_i |\alpha_i| \qquad \|\alpha\|_2 = \Big(\sum_i |\alpha_i|^2\Big)^{1/2}$$

- Solve by imposing a regularising prior that the signal to be recovered is sparse in Ψ, *i.e.* solve the following ℓ_0 optimisation problem:

$$\boxed{\boldsymbol{\alpha}^\star = \underset{\boldsymbol{\alpha}}{\arg\min} \|\alpha\|_0 \ \text{such that} \ \|\boldsymbol{y} - \Phi\Psi\boldsymbol{\alpha}\|_2 \leq \epsilon} \, ,$$

  where the signal is synthesising by $\boldsymbol{x}^\star = \Psi \boldsymbol{\alpha}^\star$.

- Solving this problem is difficult (combinatorial).

- Instead, solve the ℓ_1 optimisation problem (convex):

$$\boxed{\boldsymbol{\alpha}^\star = \underset{\boldsymbol{\alpha}}{\arg\min} \|\alpha\|_1 \ \text{such that} \ \|\boldsymbol{y} - \Phi\Psi\boldsymbol{\alpha}\|_2 \leq \epsilon} \, .$$

An introduction to compressive sensing

Promoting sparsity via ℓ_1 minimisation

- Ill-posed inverse problem:

$$\boxed{\boldsymbol{y} = \Phi \boldsymbol{x} + \boldsymbol{n} = \Phi \Psi \boldsymbol{\alpha} + \boldsymbol{n}} .$$

- Recall norms given by:

$$\|\alpha\|_0 = \text{no. non-zero elements} \qquad \|\alpha\|_1 = \sum_i |\alpha_i| \qquad \|\alpha\|_2 = \Big(\sum_i |\alpha_i|^2\Big)^{1/2}$$

- Solve by imposing a regularising prior that the signal to be recovered is sparse in Ψ, *i.e.* solve the following ℓ_0 optimisation problem:

$$\boxed{\boldsymbol{\alpha}^\star = \underset{\boldsymbol{\alpha}}{\arg\min} \|\alpha\|_0 \text{ such that } \|\boldsymbol{y} - \Phi\Psi\boldsymbol{\alpha}\|_2 \leq \epsilon} ,$$

where the signal is synthesising by $\boldsymbol{x}^\star = \Psi \boldsymbol{\alpha}^\star$.

- Solving this problem is difficult (combinatorial).

- Instead, solve the ℓ_1 optimisation problem (convex):

$$\boxed{\boldsymbol{\alpha}^\star = \underset{\boldsymbol{\alpha}}{\arg\min} \|\alpha\|_1 \text{ such that } \|\boldsymbol{y} - \Phi\Psi\boldsymbol{\alpha}\|_2 \leq \epsilon} .$$

An introduction to compressive sensing

Promoting sparsity via ℓ_1 minimisation

- Ill-posed inverse problem:

$$\boxed{\boldsymbol{y} = \Phi\boldsymbol{x} + \boldsymbol{n} = \Phi\Psi\boldsymbol{\alpha} + \boldsymbol{n}}\,.$$

- Recall norms given by:

$$\|\alpha\|_0 = \text{no. non-zero elements} \qquad \|\alpha\|_1 = \sum_i |\alpha_i| \qquad \|\alpha\|_2 = \Big(\sum_i |\alpha_i|^2\Big)^{1/2}$$

- Solve by imposing a regularising prior that the signal to be recovered is sparse in Ψ, *i.e.* solve the following ℓ_0 optimisation problem:

$$\boxed{\boldsymbol{\alpha}^\star = \arg\min_{\boldsymbol{\alpha}} \|\alpha\|_0 \ \text{ such that } \ \|\boldsymbol{y} - \Phi\Psi\boldsymbol{\alpha}\|_2 \leq \epsilon}\,,$$

where the signal is synthesising by $\boldsymbol{x}^\star = \Psi\boldsymbol{\alpha}^\star$.

- Solving this problem is difficult (combinatorial).
- Instead, solve the ℓ_1 optimisation problem (convex):

$$\boxed{\boldsymbol{\alpha}^\star = \arg\min_{\boldsymbol{\alpha}} \|\alpha\|_1 \ \text{ such that } \ \|\boldsymbol{y} - \Phi\Psi\boldsymbol{\alpha}\|_2 \leq \epsilon}\,.$$

An introduction to compressive sensing

Promoting sparsity via ℓ_1 minimisation

- Solutions of the ℓ_0 and ℓ_1 problems are often the same.
- Restricted isometry property (RIP):

$$(1-\delta_K)\|\boldsymbol{\alpha}\|_2^2 \leq \|\Theta\boldsymbol{\alpha}\|_2^2 \leq (1+\delta_K)\|\boldsymbol{\alpha}\|_2^2 \,,$$

for K-sparse $\boldsymbol{\alpha}$, where $\Theta = \Phi\Psi$.

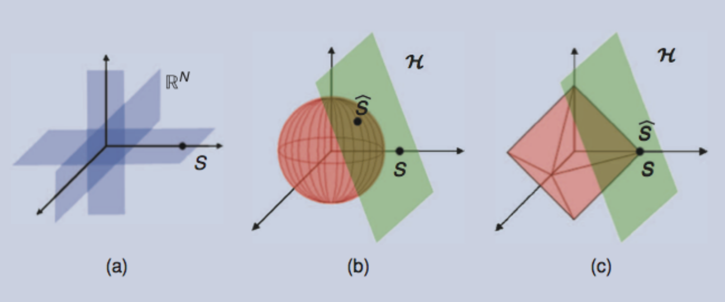

Figure: Geometry of (a) ℓ_0 (b) ℓ_2 and (c) ℓ_1 problems. [Credit: Baraniuk (2007)]

An introduction to compressive sensing

Coherence

- In the absence of noise, compressed sensing is exact!
- Number of measurements required to achieve exact reconstruction is given by

$$\boxed{M \geq c\mu^2 K \log N} \enspace ,$$

where K is the sparsity and N the dimensionality.

- The coherence between the measurement and sparsity basis is given by

$$\boxed{\mu = \sqrt{N} \max_{i,j} |\langle \Psi_i, \Phi_j \rangle|} \enspace .$$

- Robust to noise.

An introduction to compressive sensing

Coherence

- In the absence of noise, compressed sensing is exact!
- Number of measurements required to achieve exact reconstruction is given by

$$\boxed{M \geq c\mu^2 K \log N} \,,$$

where K is the sparsity and N the dimensionality.

- The coherence between the measurement and sparsity basis is given by

$$\boxed{\mu = \sqrt{N} \max_{i,j} |\langle \Psi_i, \Phi_j \rangle|} \,.$$

- Robust to noise.

An introduction to compressive sensing

Coherence

- In the absence of noise, compressed sensing is exact!
- Number of measurements required to achieve exact reconstruction is given by

$$\boxed{M \geq c\mu^2 K \log N} \, ,$$

where K is the sparsity and N the dimensionality.

- The coherence between the measurement and sparsity basis is given by

$$\boxed{\mu = \sqrt{N} \max_{i,j} |\langle \Psi_i, \Phi_j \rangle|} \, .$$

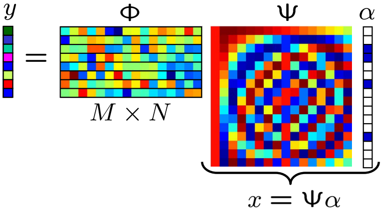

- Robust to noise.

An introduction to compressive sensing
Coherence

- In the absence of noise, compressed sensing is exact!
- Number of measurements required to achieve exact reconstruction is given by

$$\boxed{M \geq c\mu^2 K \log N} ,$$

where K is the sparsity and N the dimensionality.

- The coherence between the measurement and sparsity basis is given by

$$\boxed{\mu = \sqrt{N} \max_{i,j} |\langle \Psi_i, \Phi_j \rangle|} .$$

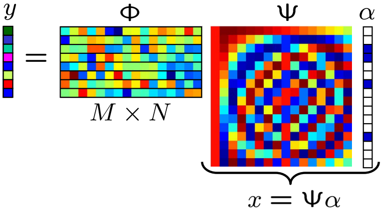

- Robust to noise.

An introduction to compressive sensing

Analysis vs synthesis

- Many new developments (*e.g.* analysis vs synthesis, cosparsity, structured sparsity).
- Synthesis-based framework:

$$\boxed{\boldsymbol{\alpha}^\star = \underset{\boldsymbol{\alpha}}{\arg\min}\, \|\boldsymbol{\alpha}\|_1 \ \text{ such that } \ \|\boldsymbol{y} - \Phi\Psi\boldsymbol{\alpha}\|_2 \leq \epsilon\,.}$$

  where we synthesise the signal from its recovered wavelet coefficients by $\boldsymbol{x}^\star = \Psi\boldsymbol{\alpha}^\star$.
- Analysis-based framework:

$$\boxed{\boldsymbol{x}^\star = \underset{\boldsymbol{x}}{\arg\min}\, \|\Psi^{\mathrm{T}}\boldsymbol{x}\|_1 \ \text{ such that } \ \|\boldsymbol{y} - \Phi\boldsymbol{x}\|_2 \leq \epsilon\,,}$$

  where the signal $\boldsymbol{x}^\star$ is recovered directly.
- Concatenating dictionaries (Rauhut *et al.* 2008) and sparsity averaging (Carrillo, McEwen & Wiaux 2013)

$$\boxed{\Psi = [\Psi_1, \Psi_2, \cdots, \Psi_q]\,.}$$

An introduction to compressive sensing

Analysis vs synthesis

- Many new developments (*e.g.* analysis vs synthesis, cosparsity, structured sparsity).
- Synthesis-based framework:

$$\boxed{\boldsymbol{\alpha}^\star = \underset{\boldsymbol{\alpha}}{\arg\min} \, \|\boldsymbol{\alpha}\|_1 \;\text{ such that }\; \|\boldsymbol{y} - \Phi\Psi\boldsymbol{\alpha}\|_2 \leq \epsilon \, .}$$

  where we synthesise the signal from its recovered wavelet coefficients by $\boldsymbol{x}^\star = \Psi\boldsymbol{\alpha}^\star$.

- Analysis-based framework:

$$\boxed{\boldsymbol{x}^\star = \underset{\boldsymbol{x}}{\arg\min} \, \|\Psi^{\mathrm{T}}\boldsymbol{x}\|_1 \;\text{ such that }\; \|\boldsymbol{y} - \Phi\boldsymbol{x}\|_2 \leq \epsilon \, ,}$$

  where the signal $\boldsymbol{x}^\star$ is recovered directly.

- Concatenating dictionaries (Rauhut *et al.* 2008) and sparsity averaging (Carrillo, McEwen & Wiaux 2013)

$$\boxed{\Psi = [\Psi_1, \Psi_2, \cdots, \Psi_q] \, .}$$

An introduction to compressive sensing

Analysis vs synthesis

- Many new developments (*e.g.* analysis vs synthesis, cosparsity, structured sparsity).
- Synthesis-based framework:

$$\boldsymbol{\alpha}^\star = \underset{\boldsymbol{\alpha}}{\arg\min} \, \|\boldsymbol{\alpha}\|_1 \;\text{ such that }\; \|\boldsymbol{y} - \Phi\Psi\boldsymbol{\alpha}\|_2 \leq \epsilon \, .$$

  where we synthesise the signal from its recovered wavelet coefficients by $\boldsymbol{x}^\star = \Psi\boldsymbol{\alpha}^\star$.

- Analysis-based framework:

$$\boldsymbol{x}^\star = \underset{\boldsymbol{x}}{\arg\min} \, \|\Psi^{\mathrm{T}}\boldsymbol{x}\|_1 \;\text{ such that }\; \|\boldsymbol{y} - \Phi\boldsymbol{x}\|_2 \leq \epsilon \, ,$$

  where the signal $\boldsymbol{x}^\star$ is recovered directly.

- Concatenating dictionaries (Rauhut *et al.* 2008) and sparsity averaging (Carrillo, McEwen & Wiaux 2013)

$$\Psi = [\Psi_1, \Psi_2, \cdots, \Psi_q] \, .$$

Interferometric imaging with compressed sensing

- Solve the interferometric imaging problem

$$\boxed{\boldsymbol{y} = \Phi \boldsymbol{x} + \boldsymbol{n} \quad \text{with} \quad \Phi = \mathbf{M}\,\mathbf{F}\,\mathbf{C}\,\mathbf{A}} \,,$$

by applying a prior on sparsity of the signal in a sparsifying dictionary Ψ.

- Basis pursuit (BP) denoising problem

$$\boldsymbol{\alpha}^\star = \underset{\boldsymbol{\alpha}}{\arg\min} \|\boldsymbol{\alpha}\|_1 \ \text{ such that } \ \|\boldsymbol{y} - \Phi\Psi\boldsymbol{\alpha}\|_2 \leq \epsilon \,,$$

where the image is synthesised by $\boldsymbol{x}^\star = \Psi\boldsymbol{\alpha}^\star$.

Interferometric imaging with compressed sensing

- Solve the interferometric imaging problem

$$\boxed{\boldsymbol{y} = \Phi \boldsymbol{x} + \boldsymbol{n} \quad \text{with} \quad \Phi = \mathbf{M}\,\mathbf{F}\,\mathbf{C}\,\mathbf{A}},$$

by applying a prior on sparsity of the signal in a sparsifying dictionary Ψ.

- Basis pursuit (BP) denoising problem

$$\boldsymbol{\alpha}^\star = \underset{\boldsymbol{\alpha}}{\arg\min} \|\alpha\|_1 \ \text{ such that } \ \|\boldsymbol{y} - \Phi\Psi\boldsymbol{\alpha}\|_2 \leq \epsilon \, ,$$

where the image is synthesised by $\boldsymbol{x}^\star = \Psi\boldsymbol{\alpha}^\star$.

SARA for radio interferometric imaging

Algorithm

- Sparsity averaging reweighted analysis (SARA) for RI imaging (Carrillo, McEwen & Wiaux 2012)

- Consider a dictionary composed of a concatenation of orthonormal bases, i.e.

$$\Psi = \frac{1}{\sqrt{q}}[\Psi_1, \Psi_2, \dots, \Psi_q],$$

  thus $\Psi \in \mathbb{R}^{N \times D}$ with $D = qN$.

- We consider the following bases: Dirac (*i.e.* pixel basis); Haar wavelets (promotes gradient sparsity); Daubechies wavelet bases two to eight.
  $\Rightarrow$ concatenation of 9 bases

- Promote average sparsity by solving the reweighted ℓ_1 analysis problem:

$$\min_{\bar{x} \in \mathbb{R}^N} \|W\Psi^T \bar{x}\|_1 \quad \text{subject to} \quad \|y - \Phi\bar{x}\|_2 \leq \epsilon \quad \text{and} \quad \bar{x} \geq 0\,,$$

  where $W \in \mathbb{R}^{D \times D}$ is a diagonal matrix with positive weights.

- Solve a sequence of reweighted ℓ_1 problems using the solution of the previous problem as the inverse weights $\rightarrow$ approximate the ℓ_0 problem.

SARA for radio interferometric imaging

Algorithm

- Sparsity averaging reweighted analysis (SARA) for RI imaging (Carrillo, McEwen & Wiaux 2012)

- Consider a dictionary composed of a concatenation of orthonormal bases, i.e.

$$\boxed{\Psi = \frac{1}{\sqrt{q}}[\Psi_1, \Psi_2, \ldots, \Psi_q],}$$

  thus $\Psi \in \mathbb{R}^{N\times D}$ with $D = qN$.

- We consider the following bases: Dirac (*i.e.* pixel basis); Haar wavelets (promotes gradient sparsity); Daubechies wavelet bases two to eight.
  $\Rightarrow$ concatenation of 9 bases

- Promote average sparsity by solving the reweighted ℓ_1 analysis problem:

$$\boxed{\min_{\bar{x}\in\mathbb{R}^N} \|W\Psi^T\bar{x}\|_1 \quad \text{subject to} \quad \|y - \Phi\bar{x}\|_2 \leq \epsilon \quad \text{and} \quad \bar{x} \geq 0\,,}$$

  where $W \in \mathbb{R}^{D\times D}$ is a diagonal matrix with positive weights.

- Solve a sequence of reweighted ℓ_1 problems using the solution of the previous problem as the inverse weights $\rightarrow$ approximate the ℓ_0 problem.

SARA for radio interferometric imaging

Algorithm

- Sparsity averaging reweighted analysis (SARA) for RI imaging (Carrillo, McEwen & Wiaux 2012)
- Consider a dictionary composed of a concatenation of orthonormal bases, i.e.

$$\boxed{\Psi = \frac{1}{\sqrt{q}}[\Psi_1, \Psi_2, \ldots, \Psi_q],}$$

thus $\Psi \in \mathbb{R}^{N \times D}$ with $D = qN$.

- We consider the following bases: Dirac (*i.e.* pixel basis); Haar wavelets (promotes gradient sparsity); Daubechies wavelet bases two to eight.
  $\Rightarrow$ concatenation of 9 bases
- Promote average sparsity by solving the reweighted ℓ_1 analysis problem:

$$\boxed{\min_{\bar{\boldsymbol{x}} \in \mathbb{R}^N} \|W\Psi^T\bar{\boldsymbol{x}}\|_1 \quad \text{subject to} \quad \|\boldsymbol{y} - \Phi\bar{\boldsymbol{x}}\|_2 \leq \epsilon \quad \text{and} \quad \bar{\boldsymbol{x}} \geq 0\,,}$$

where $W \in \mathbb{R}^{D \times D}$ is a diagonal matrix with positive weights.

- Solve a sequence of reweighted ℓ_1 problems using the solution of the previous problem as the inverse weights $\rightarrow$ approximate the ℓ_0 problem.

SARA for radio interferometric imaging

Algorithm

- Sparsity averaging reweighted analysis (SARA) for RI imaging (Carrillo, McEwen & Wiaux 2012)
- Consider a dictionary composed of a concatenation of orthonormal bases, i.e.

$$\boxed{\Psi = \frac{1}{\sqrt{q}}[\Psi_1, \Psi_2, \ldots, \Psi_q],}$$

  thus $\Psi \in \mathbb{R}^{N\times D}$ with $D = qN$.
- We consider the following bases: Dirac (*i.e.* pixel basis); Haar wavelets (promotes gradient sparsity); Daubechies wavelet bases two to eight.
  $\Rightarrow$ concatenation of 9 bases
- Promote average sparsity by solving the reweighted ℓ_1 analysis problem:

$$\boxed{\min_{\bar{\boldsymbol{x}}\in\mathbb{R}^N} \|W\Psi^T\bar{\boldsymbol{x}}\|_1 \quad \text{subject to} \quad \|\boldsymbol{y} - \Phi\bar{\boldsymbol{x}}\|_2 \leq \epsilon \quad \text{and} \quad \bar{\boldsymbol{x}} \geq 0\,,}$$

  where $W \in \mathbb{R}^{D\times D}$ is a diagonal matrix with positive weights.
- Solve a sequence of reweighted ℓ_1 problems using the solution of the previous problem as the inverse weights $\rightarrow$ approximate the ℓ_0 problem.

Supporting continuous visibilities

Algorithm

- Ideally we would like to model the continuous Fourier transform operator

$$\boxed{\Phi = \mathbf{F}^{\mathrm{c}}} \, .$$

- But this is impractically slow!
- Incorporated gridding into our CS interferometric imaging framework.
- Work of Rafael Carrillo, in collaboration with Wiaux and McEwen (see Carrillo, McEwen, Wiaux 2013).
- Model with measurement operator

$$\boxed{\Phi = \mathbf{G}\,\mathbf{F}\,\mathbf{D}\,\mathbf{Z}} \, ,$$

where we incorporate:
  - convolutional gridding operator $\mathbf{G}$;
  - fast Fourier transform $\mathbf{F}$;
  - normalisation operator $\mathbf{D}$ to undo the convolution gridding;
  - zero-padding operator $\mathbf{Z}$ to upsample the discrete visibility space.

Supporting continuous visibilities

Algorithm

- Ideally we would like to model the continuous Fourier transform operator

$$\boxed{\Phi = \mathbf{F}^{\mathrm{c}}} \,.$$

- But this is impractically slow!
- Incorporated gridding into our CS interferometric imaging framework.
- Work of Rafael Carrillo, in collaboration with Wiaux and McEwen (see Carrillo, McEwen, Wiaux 2013).
- Model with measurement operator

$$\boxed{\Phi = \mathbf{G}\,\mathbf{F}\,\mathbf{D}\,\mathbf{Z}} \,,$$

where we incorporate:
  - convolutional gridding operator $\mathbf{G}$;
  - fast Fourier transform $\mathbf{F}$;
  - normalisation operator $\mathbf{D}$ to undo the convolution gridding;
  - zero-padding operator $\mathbf{Z}$ to upsample the discrete visibility space.

Supporting continuous visibilities

Algorithm

- Ideally we would like to model the continuous Fourier transform operator

$$\boxed{\Phi = \mathbf{F}^{\mathrm{c}}} \ .$$

- But this is impractically slow!
- Incorporated gridding into our CS interferometric imaging framework.
- Work of Rafael Carrillo, in collaboration with Wiaux and McEwen (see Carrillo, McEwen, Wiaux 2013).
- Model with measurement operator

$$\boxed{\Phi = \mathbf{G}\,\mathbf{F}\,\mathbf{D}\,\mathbf{Z}} \ ,$$

where we incorporate:

  - convolutional gridding operator $\mathbf{G}$;
  - fast Fourier transform $\mathbf{F}$;
  - normalisation operator $\mathbf{D}$ to undo the convolution gridding;
  - zero-padding operator $\mathbf{Z}$ to upsample the discrete visibility space.

Supporting continuous visibilities
Results on simulations

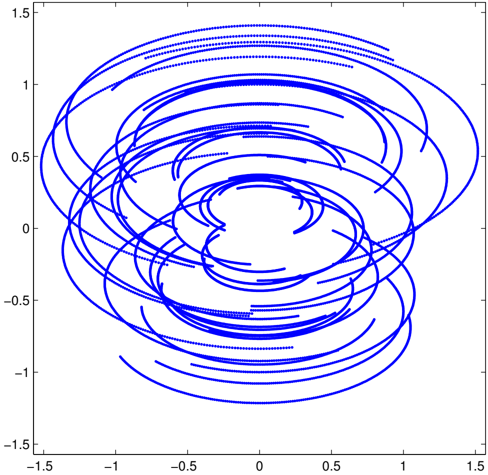

Figure: Coverage

Supporting continuous visibilities

Results on simulations

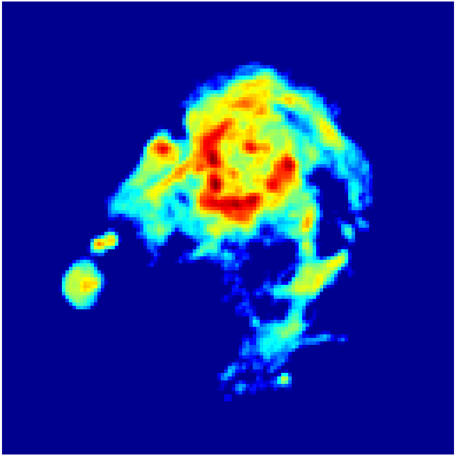

Figure: M31 (ground truth).

Supporting continuous visibilities

Results on simulations

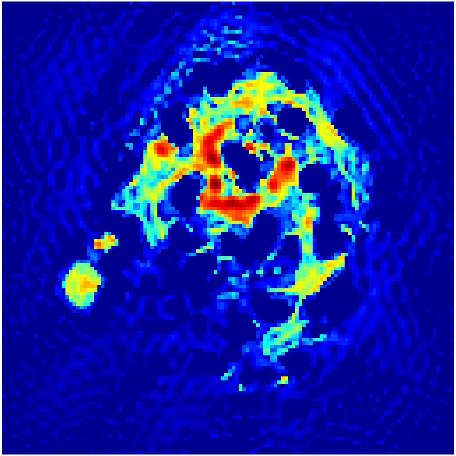

Figure: Dirac basis ("CLEAN") $\rightarrow$ SNR$= 8.2$dB.

Supporting continuous visibilities

Results on simulations

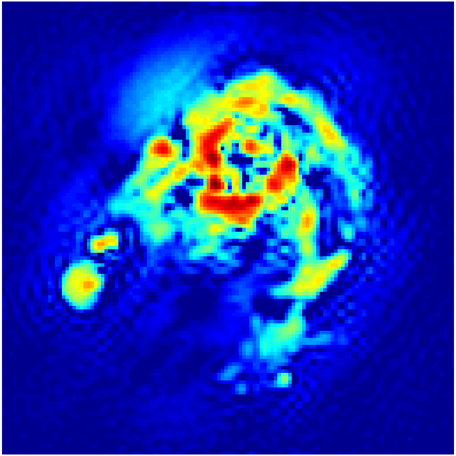

Figure: Db8 wavelets ("MS-CLEAN") $\rightarrow$ SNR$= 11.1$dB.

Supporting continuous visibilities

Results on simulations

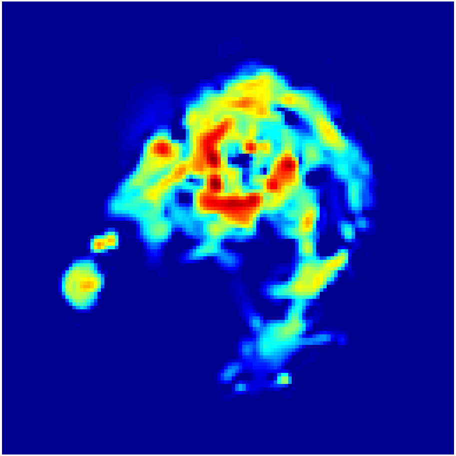

Figure: SARA $\rightarrow$ SNR$= 13.4$dB.

Outlook

- Just released the PURIFY code to scale to the realistic setting.
- Includes state-of-the-art convex optimisation algorithms that support parallelisation.
- Plan to perform more extensive comparisons with traditional techniques, such as CLEAN, MS-CLEAN and MEM.

Apply to observations made by real interferometric telescopes.

PURIFY code `http://basp-group.github.io/purify/`

Next-generation radio interferometric imaging
Carrillo, McEwen, Wiaux

PURIFY is an open-source code that provides functionality to perform radio interferometric imaging, leveraging recent developments in the field of compressive sensing and convex optimisation.

Outlook

- Just released the PURIFY code to scale to the realistic setting.
- Includes state-of-the-art convex optimisation algorithms that support parallelisation.
- Plan to perform more extensive comparisons with traditional techniques, such as CLEAN, MS-CLEAN and MEM.

Apply to observations made by real interferometric telescopes.

PURIFY code http://basp-group.github.io/purify/

Next-generation radio interferometric imaging
Carrillo, McEwen, Wiaux

PURIFY is an open-source code that provides functionality to perform radio interferometric imaging, leveraging recent developments in the field of compressive sensing and convex optimisation.

Outlook

- Just released the PURIFY code to scale to the realistic setting.
- Includes state-of-the-art convex optimisation algorithms that support parallelisation.
- Plan to perform more extensive comparisons with traditional techniques, such as CLEAN, MS-CLEAN and MEM.

Apply to observations made by real interferometric telescopes.

PURIFY code http://basp-group.github.io/purify/

Next-generation radio interferometric imaging
Carrillo, McEwen, Wiaux

PURIFY is an open-source code that provides functionality to perform radio interferometric imaging, leveraging recent developments in the field of compressive sensing and convex optimisation.

Outlook

- Just released the PURIFY code to scale to the realistic setting.
- Includes state-of-the-art convex optimisation algorithms that support parallelisation.
- Plan to perform more extensive comparisons with traditional techniques, such as CLEAN, MS-CLEAN and MEM.

Apply to observations made by real interferometric telescopes.

PURIFY code http://basp-group.github.io/purify/

Next-generation radio interferometric imaging
Carrillo, McEwen, Wiaux

PURIFY is an open-source code that provides functionality to perform radio interferometric imaging, leveraging recent developments in the field of compressive sensing and convex optimisation.

Outline

1. Dark energy
   - ISW effect
   - Continuous wavelets on the sphere
   - Detecting dark energy
2. Cosmic strings
   - String physics
   - Scale-discretised wavelets on the sphere
   - String estimation
3. Radio interferometry
   - Interferometric imaging
   - Compressive sensing
   - Imaging with CS
4. Large-scale structure
   - Wavelets on ball
   - Cosmic voids

Observations on the 3D ball

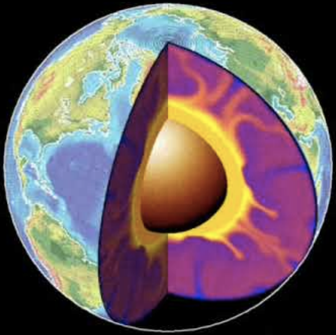

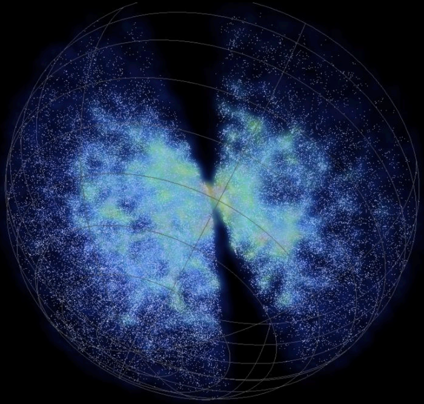

Fourier-LAGuerre wavelets (flaglets) on the ball
Construction

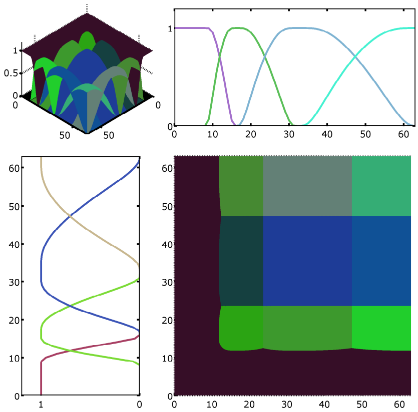

Figure: Tiling of Fourier-Laguerre space.

- *Exact wavelets on the ball* (Leistedt & McEwen 2012).
- Extend the idea of scale-discretised wavelets on the sphere (Wiaux, McEwen, Vandergheynst, Blanc 2008) to the ball.
- Construct wavelets by tiling the ℓ–p harmonic plane.
- Scale-discretised wavelet $\Psi^{jj'} \in \mathrm{L}^2(B^3)$ is defined in harmonic space:

$$\Psi^{jj'}_{\ell mp} \equiv \sqrt{\frac{2\ell+1}{4\pi}}\,\kappa_\lambda(\ell\lambda^{-j})\kappa_\nu(p\nu^{-j'})\delta_{m0}.$$

- Construct wavelets to satisfy a resolution of the identity:

$$\frac{4\pi}{2\ell+1}\Bigg(\underbrace{\boxed{|\Phi_{\ell 0p}|^2}}_{\text{scaling function}}+\sum_{j=J_0}^{J}\sum_{j'=J'_0}^{J'}\underbrace{\boxed{|\Psi^{jj'}_{\ell 0p}|^2}}_{\text{wavelet}}\Bigg) = 1, \forall \ell, p.$$

Fourier-LAGuerre wavelets (flaglets) on the ball

Construction

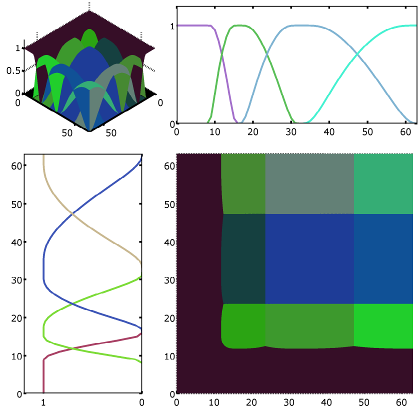

Figure: Tiling of Fourier-Laguerre space.

- *Exact wavelets on the ball* (Leistedt & McEwen 2012).
- Extend the idea of scale-discretised wavelets on the sphere (Wiaux, McEwen, Vandergheynst, Blanc 2008) to the ball.
- Construct wavelets by tiling the ℓ–p harmonic plane.
- Scale-discretised wavelet $\Psi^{jj'} \in \mathrm{L}^2(B^3)$ is defined in harmonic space:

$$\Psi^{jj'}_{\ell mp} \equiv \sqrt{\frac{2\ell+1}{4\pi}}\,\kappa_\lambda(\ell\lambda^{-j})\kappa_\nu(p\nu^{-j'})\delta_{m0}.$$

- Construct wavelets to satisfy a resolution of the identity:

$$\frac{4\pi}{2\ell+1}\left(\underbrace{\boxed{|\Phi_{\ell 0p}|^2}}_{\text{scaling function}}+\sum_{j=J_0}^{J}\sum_{j'=J'_0}^{J'}\underbrace{\boxed{|\Psi^{jj'}_{\ell 0p}|^2}}_{\text{wavelet}}\right) = 1, \forall \ell, p.$$

Fourier-LAGuerre wavelets (flaglets) on the ball

Wavelets

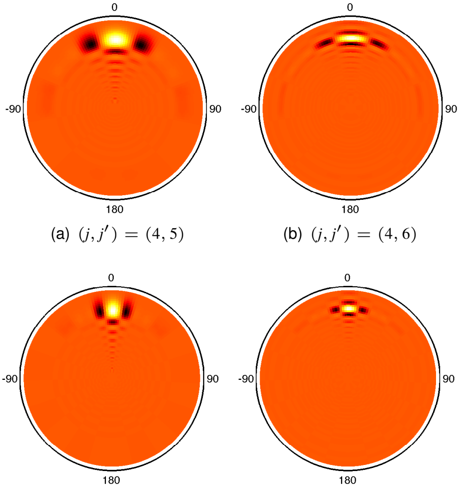

(a) $(j, j') = (4, 5)$ (b) $(j, j') = (4, 6)$

(c) $(j, j') = (5, 5)$ (d) $(j, j') = (5, 6)$

Fourier-LAGuerre wavelets (flaglets) on the ball

Wavelets

Wavelets

Fourier-LAGuerre wavelets (flaglets) on the ball

Forward and inverse transform (*i.e.* analysis and synthesis)

- The Fourier-Laguerre wavelet transform is given by the usual projection onto each wavelet:

$$\underbrace{\boxed{W^{\Psi^{jj'}}(\boldsymbol{r}) = (f \star \langle f | \mathcal{T}_{\boldsymbol{r}} \Psi^{jj'} \rangle_{\mathbb{B}^3}}}_{\text{projection}} = \int_{B^3} \mathrm{d}^3\boldsymbol{r}' f(\boldsymbol{r}')(\mathcal{T}_{\boldsymbol{r}}\Psi^{jj'})(\boldsymbol{r}') \; .$$

- The original function may be synthesised exactly in practice from its wavelet (and scaling) coefficients:

$$f(\boldsymbol{r}) = \underbrace{\boxed{\int_{B^3} \mathrm{d}^3\boldsymbol{r}' W^{\Phi}(\boldsymbol{r}')(\mathcal{T}_{\boldsymbol{r}}\Phi)(\boldsymbol{r}')}}_{\text{scaling function contribution}} + \underbrace{\boxed{\sum_{j=J_0}^{J} \sum_{j'=J'_0}^{J'}}}_{\text{finite sum}} \underbrace{\boxed{\int_{B^3} \mathrm{d}^3\boldsymbol{r}' W^{\Psi^{jj'}}(\boldsymbol{r}')(\mathcal{T}_{\boldsymbol{r}}\Psi^{jj'})(\boldsymbol{r}') \; .}}_{\text{wavelet contribution}}$$

Fourier-LAGuerre wavelets (flaglets) on the ball

Forward and inverse transform (*i.e.* analysis and synthesis)

- The Fourier-Laguerre wavelet transform is given by the usual projection onto each wavelet:

$$\underbrace{\boxed{W^{\Psi^{jj'}}(\boldsymbol{r}) = (f \star \langle f | \mathcal{T}_{\boldsymbol{r}} \Psi^{jj'} \rangle_{\mathbb{B}^3}}}_{\text{projection}} = \int_{B^3} \mathrm{d}^3\boldsymbol{r}' f(\boldsymbol{r}')(\mathcal{T}_{\boldsymbol{r}}\Psi^{jj'})(\boldsymbol{r}') \, .$$

- The original function may be synthesised exactly in practice from its wavelet (and scaling) coefficients:

$$f(\boldsymbol{r}) = \underbrace{\boxed{\int_{B^3} \mathrm{d}^3\boldsymbol{r}' \, W^{\Phi}(\boldsymbol{r}')(\mathcal{T}_{\boldsymbol{r}}\Phi)(\boldsymbol{r}')}}_{\text{scaling function contribution}} + \underbrace{\boxed{\sum_{j=J_0}^{J} \sum_{j'=J_0'}^{J'}}}_{\text{finite sum}} \underbrace{\boxed{\int_{B^3} \mathrm{d}^3\boldsymbol{r}' \, W^{\Psi^{jj'}}(\boldsymbol{r}')(\mathcal{T}_{\boldsymbol{r}}\Psi^{jj'})(\boldsymbol{r}') \, .}}_{\text{wavelet contribution}}$$

Fourier-LAGuerre wavelets (flaglets) on the ball

Exact and efficient computation

- For a band-limited signal, we can compute Fourier-Laguerre wavelet transforms exactly.

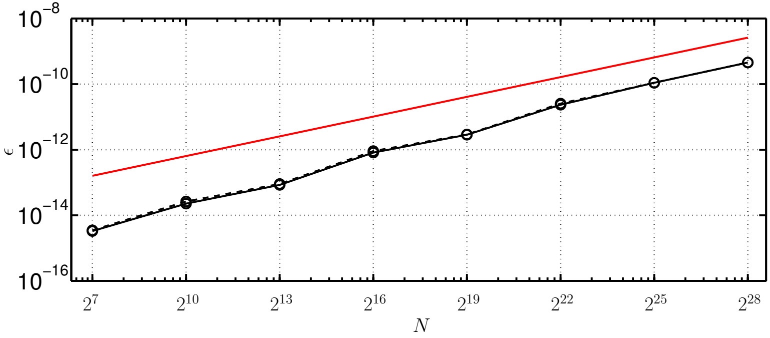

Figure: Numerical accuracy of the flaglet transform.

Fourier-LAGuerre wavelets (flaglets) on the ball

Exact and efficient computation

- Fast algorithms to compute Fourier-Laguerre wavelet transforms.

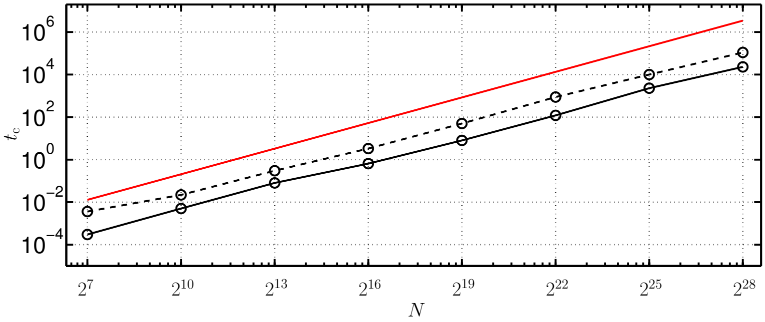

Figure: Computation time of the flaglet transform.

Fourier-LAGuerre wavelets (flaglets) on the ball

Codes

FLAGLET code http://www.flaglets.org

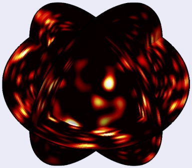

Exact wavelets on the ball
Leistedt & McEwen (2012)

- C, Matlab
- Exact (Fourier-LAGuerre) wavelets on the ball – coined *flaglets*!

FLAG code http://www.flaglets.org

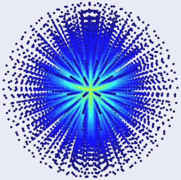

FLAG: Fourier-Laguerre trnasform on the ball
Leistedt & McEwen (2012)

- C, Matlab

Analysis of large-scale structure (LSS)

- Map Horizon simulation of large-scale structure (LSS) to Fourier-Laguerre sampling.

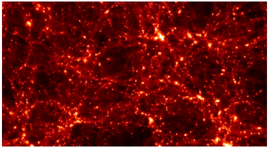

LSS fly through

Flaglet void finding

- Find voids in the large-scale structure (LSS) of the Universe.
- Perform Alcock & Paczynski (1979) test: study void shapes to constrain the nature of dark energy (*e.g.* Sutter *et al.* 2012).

LSS voids

Summary

A rapid tour of sparsity, wavelets, compressive sensing and all that . . .

. . . and their application to cosmology.

Summary

A rapid tour of sparsity, wavelets, compressive sensing and all that . . .

. . . and their application to cosmology.

Application of informatics techniques like wavelets for CMB analysis well-established.

Summary

A rapid tour of sparsity, wavelets, compressive sensing and all that . . .

. . . and their application to cosmology.

Application of informatics techniques like wavelets for CMB analysis well-established.

Great potential to exploit informatics techniques for analysis of LSS!